Graduate School ETD Form 9
(Revised 01/14)

PURDUE UNIVERSITY
GRADUATE SCHOOL
Thesis/Dissertation Acceptance

This is to certify that the thesis/dissertation prepared

By Yiting Hao

Entitled
VISIBLE LIGHT CURED THIOL-VINYL HYDROGELS WITH TUNABLE GELATION AND DEGRADATION

For the degree of Master of Science in Biomedical Engineering

Is approved by the final examining committee:

Chien-Chi Lin

Dong Xie

Tien-Min Gabriel Chu

To the best of my knowledge and as understood by the student in the *Thesis/Dissertation Agreement. Publication Delay, and Certification/Disclaimer (Graduate School Form 32)*, this thesis/dissertation adheres to the provisions of Purdue University's "Policy on Integrity in Research" and the use of copyrighted material.

Chien-Chi Lin

Approved by Major Professor(s): _____

_____

Approved by: Edward Berbari 04/29/2014

Head of the Department Graduate Program Date

VISIBLE LIGHT CURED THIOL-VINYL HYDROGELS WITH TUNABLE GELATION AND DEGRADATION

A Thesis

Submitted to the Faculty

of

Purdue University

by

Yiting Hao

In Partial Fulfillment of the

Requirements for the Degree

of

Master of Science in Biomedical Engineering

May 2014

Purdue University

Indianapolis, Indiana

ACKNOWLEDGMENTS

First and foremost, I would like to express the deepest appreciation to my advisor, Dr. Chien-chi Lin, who has been a tremendous mentor for me. I would like to thank him for his excellent guidance, caring, patience, and providing me with an excellent atmosphere for doing research. I feel grateful for his fully support during my master education.

Second, I would like to thanks my committee members, Dr. Dong Xie, and Dr. Tien-min Gabriel Chu, for their time and insight during the completion of this thesis.

I would also like to extend my special thanks to my co-workers in the laboratory, Dr. Chang Seok Ki, Dr. Tsai-Yu Lin, Ms. Han Shih, Ms. Tanja Greene and Mr. Zachary Munoz for their help, suggestion and support during my research. I also want to thank Ms. Valerie Lim Diemer for assisting me in formatting this thesis.

Finally, a special thanks to my parents and my friends, who provide help and support during all my life. The product of this research thesis would not be possible without them.

TABLE OF CONTENTS

Page

Page

LIST OF TABLES

LIST OF FIGURES

Figure Page

Figure Page

Figure Page

SYMBOLS

γ	Applied shear
ε	Molar absorption coefficient, $M^{-1}cm^{-1}$
ξ	Mesh size, nm
ρ_1	Solvent density, g/cm^3
ρ_2	Polymer density, g/cm^3
σ	Shear stress, Pa
χ_{12}	Polymer-solvent interaction parameter
C_n	Flory characteristic ratio
G'	Elastic or (storage) modulus, Pa
G''	Viscous or (loss) modulus, Pa
k_{hyd}	Degradation rate constant, day^{-1}
l	Average bond length along the polymer backbone, Å
$\overline{M_c}$	Average molecular weight between crosslinks, Da
$\overline{M_n}$	Average molecular weight of the polymer chain, Da
M_r	Molecular weight of the repeating units, Da
n	Number of bonds between adjacent crosslinks
Q_m	Mass swelling ratio
Q_v	Volume swelling ratio
R	Gas constant, $Jmol^{-1}K^{-1}$
T	Absolute temperature, K
$v_{2,s}$	Polymer volume fraction in the swollen state
$\overline{v}$	Specific volume of the polymer, cm^3/g
V_1	Molar volume of water, cm^3/mol
V_g	Swollen gel volume, cm^3

V_p	Dried gel volume, cm^3
W_{dry}	Dried polymer weight, mg
$W_{swollen}$	Swollen gel weight, mg

ABBREVIATIONS

Ac-CRGDS	Acetylated modified 5-mer peptide
Acryl-RGDS	Acrylated modified 4-mer peptide
DTT	Dithiothreitol
ECM	Extracellular matrix
HPLC	High performance liquid chromatography
KCGPQGIWGQCK	MMP-sensitive 12-mer peptide
KCGPQGPAGQCK	Non MMP-sensitive 12-mer peptide
LAP	Lithium phenyl-2,4,6-trimethyl-benzoylphosphinate
LCST	Lower critical solution temperature
MBA	N,N'-methylenebis(acrylamide)
NVP	1-vinyl-2-pyrrolidinone
PCL	Poly(ϵ-caprolactone)
PEG	Poly(ethylene glycol)
PEG2SH	Poly(ethylene glycol)-di-thiol
PEG4A	Poly(ethylene glycol)-tetra-acrylate
PEG4AA	Poly(ethylene glycol)-tetra-acrylamide
PEG4AE	Poly(ethylene glycol)-tetra-allylether
PEG4MA	Poly(ethylene glycol)-tetra-methacrylate
PEGDA	Poly(ethylene glycol)-diacrylate
PGA	Poly(glycolic acid)
PHEMA	Poly(hydroxyethyl methacrylate)
PLA	Poly(lactic acid)
PNIPAm	Poly(N-isopropylacrylamide)
PVA	Poly(vinyl alcohol)

RGD	3-mer peptide arginine-glycine-aspartic acid
TEA	Triethanolamine
TEGDMA	Tetraethylene glycol dimethacrylate

ABSTRACT

Hao, Yiting. M.S.B.M.E, Purdue University, May 2014. Visible Light Cured Thiol-vinyl Hydrogels with Tunable Gelation and Degradation. Major Professor: Chien-Chi Lin.

Hydrogels prepared from photopolymerization have been widely used in many biomedical applications. Ultraviolet (200-400 nm) or visible (400-800 nm) light can interact with light-sensitive compounds called photoinitiators to form radical species that trigger photopolylmerization. Since UV light has potential to cause cell damage, visible light-mediated photopolymerization has attracted much attention. The conventional method to fabricate hydrogels under visible light exposure requires usage of co-initiator triethanolamine (TEA) at high concentration ($\sim$200 mM), which reduces cell viability. Therefore, the first objective of this thesis was to develop a new method to form poly(ethylene glycol)-diacrylate (PEGDA) hydrogel without using TEA. Specifically, thiol-containing molecules (e.g. dithiothreitol or cysteine-containing peptides) were used to replace TEA as both co-initiator and crosslinker. Co-monomer 1-vinyl-2-pyrrolidinone (NVP) was used to accelerate gelation kinetics. The gelation rate could be tuned by changing the concentration of eosinY or NVP. Variation of thiol concentration affected degradation rate of hydrogels. Many bioactive motifs have been immobilized into hydrogels to enhance cell attachment and adhesion in previous studies. In this thesis, pendant peptide RGDS was incorporated via two methods with high incorporation efficiency. The stiffness of hydrogels decreased when incorporating RGDS. The second objective of this thesis was to fabricate hydrogels using poly(ethylene glycol)-tetra-acrylate (PEG4A) macromer instead of PEGDA via the same step-and-chain-growth mixed mode mechanism. Formation of hydrogels using PEGDA in this thesis required high concentration of macromer

($\sim$10 $wt.\%$). Since PEG4A had two more functional acrylate groups than PEGDA, hydrogels could be fabricated using lower concentration of PEG4A ($\sim$4 $wt.\%$). The effects of NVP concentration and thiol content on hydrogel properties were similar to those on PEGDA hydrogels. In addition, the functionality and chemistry of thiol could also affect hydrogel properties.

1. INTRODUCTION

1.1 Hydrogels

The application of hydrogels dates back to 1960, when Professors Lim and Wichterle first synthesized poly-2-hydroxyethyl methacrylate hydrogel for soft contact lens [1]. Since then, the number of papers related with topic of hydrogels has increased exponentially [2,3]. The reasons why hydrogels attract such attention are that they exhibit excellent biocompatibility and have good permeability for nutrients and oxygen. Hydrogels are hydrophilic, cross-linked polymeric network and can absorb substantial amounts of water without dissolution. Hydrogels also have physical properties that are similar to soft tissues. Due to these advantages, hydrogels have been extensively used in biomedical applications [3], such as contact lens, biosensors, absorbable sutures, wound dressing and cell transplantation as well as drug delivery.

1.1.1 Hydrogel from Natural and Synthetic Materials

Hydrogels can be made from natural polymers including collagen, gelatin, fibrin, hyaluronic acid, alginate, agarose, chitosan, and so on [4]. Collagen is a major component in extracellular matrices of mammalian tissues and can be chemically cross-linked using glutaraldehyde [5] or diphenylphosphoryl azide [6]. Gelatin is a derivative of collagen, formed by breaking the natural triple-helix structure of collagen into single-strand molecule. Gelatin and collagen are temperature-sensitive materials that can easily form gels by changing the temperature of its solution [7]. Hyaluronic acid is one of the glycosaminoglycan components in natural extracellular matrices. Modified hyaluronic acid can form hydrogels through addition reaction or condensation reaction [8]. Fibrin hydrogel can be fabricated through enzymatic polymerization

of fibrinogen in the present of thrombin at room temperature. Incorporation with bioactive peptides makes fibrin gels able to bind with heparin, fibronectin, and integrins [9]. Alginate is another well-known biomaterial, which is a polysaccharide isolated from brown algae, and can be crosslinked with chelating cations (e.g., Ca^{2+} or Ba^{2+}) through ionic interaction [10]. Agarose is another type of polysaccharide that obtained from marine seaweed and can form reversible gels through non-covalent interactions [11]. Chitosan is a linear polysaccharide derived from chitin and can form hydrogels through ionic interaction [12]. Chitosan functionalized with azide and lactose moieties can be crosslinked by UV irradiation [13]. Although usually exhibiting excellent biocompatibility, hydrogels fabricated by natural derived polymers typically possess low mechanical properties and variations between batches. In contrast, synthetic polymers can be prepared with precisely controlled and reproducible structure and properties [14]. Figure 1.1 shows chemical structures of several synthetic polymers that are used to fabricate hydrogels.

Poly(hydroxyethyl methacrylate) (polyHEMA, PHEMA) is one of the most important and most widely applied hydrogels. PolyHEMA was first synthesized in 1960 [1] and after that it has been modified with many natural and synthetic substances [15–17]. One way to prepare polyHEMA hydrogel is photopolymerization using 2-hydroxyethyl methacrylate (HEMA) as the monomer, tetraethylene glycol dimethacrylate (TEGDMA) as the crosslinking agent, and Irgacure 651 as the photoinitiator [18]. Poly(vinyl alcohol) (PVA) hydrogels are distinguished by their good mechanical properties through alternating cycles of freezing and thawing [19]. Acrylate modified PVA can be crosslinked using UV radiation [20]. The PVA hydrogels formed via freezing and thawing method usually have greater mechanical strength [21]. Poly(N-isopropylacrylamide) (PNIPAm) has been investigated extensively as it exhibits phase transition behavior at the lower critical solution temperature (LCST) 32°C. Therefore, PNIPAm hydrogels can be formed when warming up to body temperature. This polymer can also form thermosensitive hydrogels from free radical

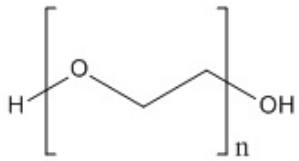

(a) Poly(ethylene glycol)

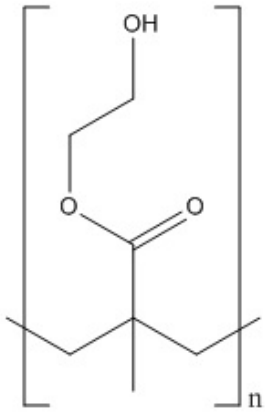

(b) Poly(hydroxylethyl methacrylate)

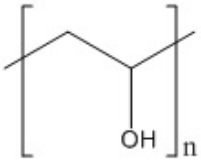

(c) Poly(vinyl alcohol)

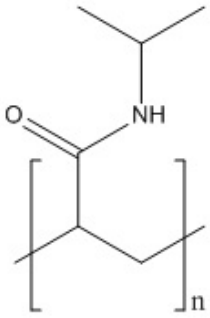

(d) Poly(N-isopropylacrylamide)

Fig. 1.1. Structure of several synthetic polymers

copolymerizing of NIPAm with crosslinkers such as N,N'-methylenebis(acrylamide) (MBA) [22].

FDA has approved several medical devices containing poly(ethylene glycol) (PEG) [23] due to its high biocompatibility, lack of toxic influence on surrounding tissue and high solubility in water. The materials used in this thesis were PEG and its derivatives. One of the common methods to functionalize PEG is the modification of terminal hydroxyl group into other active functional groups [24]. Among many PEG derivatives, vinyl-based PEG macromers are commonly used, including PEG-methacrylate (Figure 1.2(c)) [25,26], PEG-acrylate (Figure 1.2(a) and (d)) [27–29], PEG-allylether

(Figure 1.2(b)) [30], PEG-acrylamide (Figure 1.2(e)) [31, 32], PEG-maleimide (Figure 1.2(f)) [33], PEG-norbornene (Figure 1.2(g)) [34] and PEG-vinylsulfone (Figure 1.2(h)) [35, 36]. PEG hydrogels could be fabricated through chain-growth polymerization. For example, Ward and Peppas [37] fabricated hydrogels using PEG-dimethacrylate via UV free-radical chain-growth photopolymerization. PEG-acrylate has also been investigated to form hydrogels containing Arg-Gly-Asp (RGD) motifs through chain-growth polymerization [38, 39]. Elbert and Hubbell [31] developed a non-degradable hydrogel using PEG-acrylamide as macromer via chain-growth polymerization. Another alternative method to form hydrogels is step-growth polymerization. For example, Hubbell's group [40] has developed a method to crosslink multi-armed PEG-acrylate with thiol-containing molecules via a step-growth nucleophilic reaction, also called Michael-type addition reaction. The formation of hydrogels was achieved via the Michael-type addition of maleimide and thiol-terminated PEG macromers [41]. PEG-vinylsulfone could react with cysteine-containing peptides via Michael addition [42]. Many previous researches have reported that PEG-norbornene can form hydrogels via a radical-mediated thiol-ene step-growth photopolymerization [34, 43, 44]. In addition, hydrogels can be prepared through mixed-mode chain-and-step-growth photopolymerization. For example, Reddy et al. [45] have investigated degradable thiol-acrylate networks formed via copolymerizing thiol monomers with PLA-*b*-PEG-*b*-PEG based diacrylate macromers. Under UV light exposure, Salinas and Anseth [46] fabricated hydrogels using PEG-diacrylate and thiol-containing peptides via mixed mode thiol-acrylate photopolymerization.

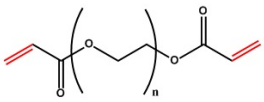

(a) PEG-diacrylate

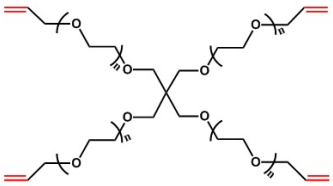

(b) PEG-tetra-allylether

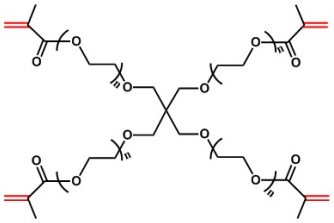

(c) PEG-tetra-methacrylate

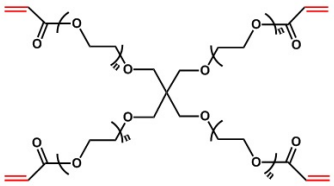

(d) PEG-tetra-acrylate

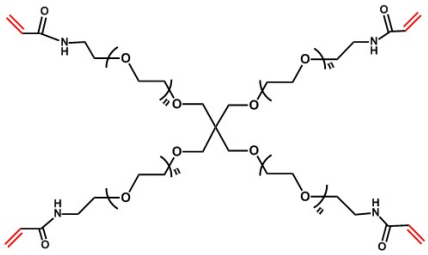

(e) PEG-tetra-acrylamide

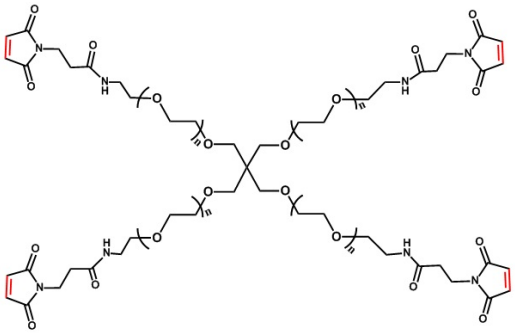

(f) PEG-tetra-maleimide

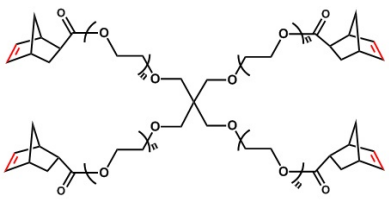

(g) PEG-tetra-norbornene

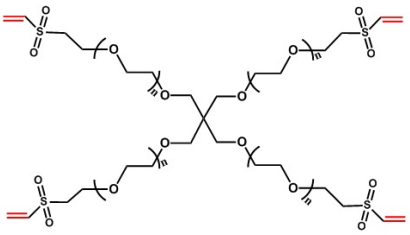

(h) PEG-tetra-vinylsulfone

Fig. 1.2. Structure of several PEG derivatives

1.1.2 Swelling of Synthetic Hydrogels

Crosslinked polymer hydrogels swell but not dissolve when absorb a large amount of water. Two common methods to evaluate the swelling property of hydrogels are to compare dry and swollen weight through mass swelling ratio Q_m or to compare dry and swollen volume through volume swelling ratio Q_v. They can be defined by the following equations:

$$Q_m = \frac{W_{swollen}}{W_{dry}} \tag{1.1}$$

and

$$Q_v = \frac{V_g}{V_p} = \frac{Q_w/\rho_1 + 1/\rho_2}{1/\rho_2} \tag{1.2}$$

where $W_{swollen}$ is the swollen gel weight, W_{dry} is the dried polymer weight, V_g is the swollen gel volume, V_p is the polymer volume, ρ_1 is the solvent density, and ρ_2 is the polymer solution density.

Another important parameter to describe the swelling property of hydrogel is the polymer volume fraction in the swollen state ($\upsilon_{2,s}$), which describes the amount of solvent absorbed by the hydrogels. It equals to the ratio of the polymer volume (V_p) to the swollen gel volume (V_g).

$$\upsilon_{2,s} = \frac{V_p}{V_g} = \frac{1}{Q_v} \tag{1.3}$$

The average molecular weight between crosslinks $\overline{M_c}$ represents the degree of hydrogel network crosslinking. According to Flory-Rehner Equation [47], in a neutral network, $\overline{M_c}$ can be described as:

$$\frac{1}{\overline{M_c}} = \frac{2}{\overline{M_n}} - \frac{(\frac{\overline{v}}{V_1})[\ln(1-\upsilon_{2,s}) + \upsilon_{2,s} + \chi_{12}\upsilon_{2,s}^2]}{\upsilon_{2,s}^{1/3} - \frac{\upsilon_{2,s}}{2}} \tag{1.4}$$

Here, $\overline{M_n}$ is the number average molecular weight of the polymer chain, $\overline{v}$ is the specific volume of the polymer in the amorphous state, V_1 is the molar volume of water (for water, it is 18 cm^3/mol), and χ_{12} is the polymer-solvent interaction parameter (0.426 for PEG-water [48]).

To determine network mesh size (ξ), the root-mean-squared end-to-end distance of network chains between two adjacent crosslinks in the unperturbed state ($(\overline{r_0}^2)^{1/2}$) is calculated using the following equation:

$$(\overline{r_0}^2)^{1/2} = lC_n^{1/2}n^{1/2} = l(C_n\frac{3\overline{M_c}}{M_r})^{1/2} \tag{1.5}$$

where l is the average bond length along the polymer backbone (0.146 nm), C_n is the characteristic ratio, n is the number of bonds between adjacent crosslinks, and M_r is the molecular mass of the polymer repeat unit (44 g/mol for PEG). Mesh size, which is defined as the linear distance between two adjacent crosslinks, can then be calculated by [49]:

$$\xi = \upsilon_{2,s}^{-1/3}(\overline{r_0}^2)^{1/2} \tag{1.6}$$

The degree of crosslinking is one of the most important factors that affect swelling of hydrogels. In general, highly crosslinked hydrogels possess tighter network and swell less. The chemical structures of polymers also influence the swelling property of hydrogels. Hydrogels containing hydrophobic motifs usually swell less compared with those containing hydrophilic motifs. The swelling property can also be affected by external stimuli, such as temperature, pH and ionic strength [50, 51]. Swelling of temperature-sensitive hydrogels can be tuned by changing the temperature of swelling media [52]. pH-sensitive and ionic strength sensitive hydrogels exhibit different swelling properties in media with different pH values and ion concentrations respectively [53, 54].

1.1.3 Mechanical Property of Synthetic Hydrogels

Mechanical property of hydrogels is very important for many biomedical applications. For example, a drug delivery system should have the ability to maintain its integrity to protect sensitive therapeutic agents until they are released from the system [51]. Encapsulated cells in hydrogels with different mechanical property express different phenotypes. Therefore, the stiffness of hydrogels plays an important role in the proliferation and differentiation of encapsulated cells [55, 56].

One common method used to get quantitative information on viscoelastic and rheological properties of hydrogels is dynamic mechanical analysis [57]. In this analysis, the sample is deformed under periodic strain. Typical input and response curves are shown in Figure 1.3. In the dynamic mechanical testing, if applied shear strain is an oscillatory function of time with frequency ω and maximum amplitude γ_m, that is

$$\gamma(t) = \gamma_m \sin(\omega t) \tag{1.7}$$

Then the shear stress as response is usually in the form:

$$\sigma(t) = \sigma_m \sin(\omega t + \delta) \tag{1.8}$$

$$= (\sigma_m \cos\delta) \sin(\omega t) + (\sigma_m \sin\delta) \cos(\omega t) \tag{1.9}$$

with a maximum amplitude σ_m and a shifted phase angle δ.

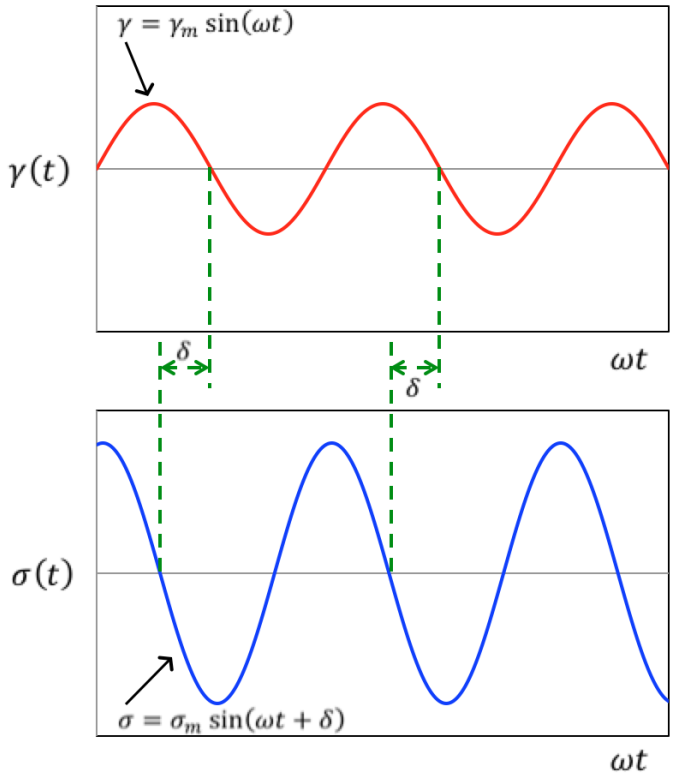

Fig. 1.3. Typical input-response curves during dynamic mechanical analysis [57]

The stress (σ) can be decomposed into two components, one in phase with the strain ($\sin\omega t$) and one out of phase by $90°(\cos\omega t)$, that is

$$\sigma = \sigma'_m \sin(\omega t) + \sigma''_m \cos(\omega t) \tag{1.10}$$

Compare the equations 1.9 and 1.10, leading to

$$\sigma'_m = \sigma_m \cos\delta \tag{1.11}$$

and

$$\sigma''_m = \sigma_m \sin\delta \tag{1.12}$$

Therefore, two dynamic modulus, elastic (or storage) modulus G' and viscous (or loss) modulus G'' can be defined as following equations:

$$G' = \frac{\sigma'_m}{\gamma_m} = \frac{\sigma_m \cos\delta}{\gamma_m} \tag{1.13}$$

and

$$G'' = \frac{\sigma''_m}{\gamma_m} = \frac{\sigma_m \sin\delta}{\gamma_m} \tag{1.14}$$

The storage modulus (G') describes the elastic character or the energy stored in the material during deformation, while loss modulus (G'') gives information about viscosity or the energy dissipated as heat. The point where G' surpasses G'' during hydrogel gelation is called the gel point. After gel formation, equilibrium storage modulus G' determines the stiffness of hydrogels. Hydrogels in swollen state usually satisfy the theory of rubber elasticity [57]. Therefore, the elastic modulus of common hydrogels is related to the swelling property through the following equation:

$$G' = \frac{\rho_2 RT}{\overline{M_c}}(1 - \frac{2\overline{M_c}}{\overline{M_n}})(\upsilon_{2,s})^{1/3} = \frac{\rho_2 RT}{\overline{M_c}}(1 - \frac{2\overline{M_c}}{\overline{M_n}})\frac{1}{Q_v^{1/3}} \tag{1.15}$$

where R is the gas constant ($8.31\ Jmol^{-1}K^{-1}$) and T is the absolute temperature.

One way to achieve the desired mechanical property is changing the degree of crosslinking [57]. However, there is a limitation using this method, as higher crosslinking density also leads to brittleness and less elasticity. In addition, high degree of crosslinking decreases the permeability of hydrogels, which makes harsh environment for encapsulated cells to survive. In this thesis, several other methods were used to regulate stiffness of hydrogels, which will be discussed in further chapters.

1.1.4 Hydrolytic Degradability of Synthetic Hydrogels

Biodegradability is one of the most important considerations of scaffolds for tissue engineering [36]. For the application in implantation, hydrogels have been developed to be biodegradable in order to avoid second surgery for taking them out. Degradable hydrogels can be degraded and ultimately absorbed by the body after tissue is regenerated [51]. The degradation of hydrogel is also a critical issue in tissue engineering [55], which should match with the timeline of tissue development and regeneration.

Hydrogels can be degraded hydrolytically or enzymatically [33]. All PEG-based hydrogels fabricated in this thesis degraded hydrolytically. Typical polymer bonds that can undergo hydrolytically degradation are anhydride, ortho-ester, thiolether-ester, ketal, acetal, hydroxyl ester and caprolactone [58]. Polyesters have been incorporated in biodegradable polymers such as poly(lactic acid) (PLA), poly(glycolic acid) (PGA), poly(ϵ-caprolactone) (PCL) and their copolymers [59]. Pure PEG is chemically stable and cannot be hydrolyzed under physiological conditions. However, with modification to form acrylated PEG macromers, they can be fabricated into biodegradable hydrogels via chemical crosslinking. For example, triblock copolymer, PLA-PEG-PLA diarylate can be photopolymerized to form hydrolytically degradable hydrogels [60]. Biodegradable PEG hydrogels can also be fabricated using PEG-acrylate with thiol-containing molecule through Michael type addition reaction [40] or UV-based photopolymerization [61]. Such hydrogels are hydrolytically degradable because they introduce thioether-ester bonds into network after polymerization. Thioether-ester bond is much more susceptible to hydrolytic degradation compared to unmodified ester bond [58].

In general, there are two types of hydrolytic degradation, surface erosion and bulk degradation [62]. In surface erosion, the polymer degrades from the exterior surface. The inside of polymer does not degrade until the outer layer material around it has been degraded. In bulk degradation, degradation occurs throughout the whole material equally. PEG-based hydrogels formed in this thesis are degraded via bulk

degradation mechanism [40]. Mathematically, the hydrolysis of labile ester bonds can be expressed as:

$$-\frac{d[Ester]}{dt} = k[Ester][H_2O] \tag{1.16}$$

where $[Ester]$ is the concentration of ester bonds in the polymer, t is the degradation time, k is the kinetic rate constant, and $[H_2O]$ is the concentration of water, which is often considered constant for simplification. Therefore, equation 1.16 can be simplified as:

$$-\frac{d[Ester]}{dt} = k'[Ester] \tag{1.17}$$

Here, k' is a pseudo-first order rate constant. Integrating equation 1.17 yields:

$$\frac{[Ester]}{[Ester]_0} = e^{-k't} \tag{1.18}$$

where $[Ester]_0$ is the initial ester bond concentration. Since $[Ester]$ is related to the molecular weight (M_n) of the polymer at any time during degradation, equation 1.18 can also be written as:

$$\frac{M_n}{M_{n0}} = e^{-k't} \tag{1.19}$$

where M_{n0} is the initial molecular weight of the polymer.

In addition, assuming a high swelling ratio ($Q > 10$), the Flory-Rehner equation 1.4 can be substituted into equation 1.15:

$$G' = \frac{\rho_2 RT}{\overline{M_c}} \frac{1}{[\beta(\overline{M_c}^{3/5})]^{1/3}} = \frac{\gamma}{\overline{M_c}^{6/5}} \tag{1.20}$$

where β and γ are constants. According to previous research [63], $\overline{M_c}$ increases exponentially with time. Therefore, based on equation 1.20, elastic modulus G' should decrease exponentially as function of time.

1.1.5 Biomimetic Hydrogels

In native tissues, cell attachment to extracellular matrix (ECM) is prerequisite for many cell activities, such as cell proliferation and migration [64]. The major limitation of synthetic materials as scaffolds for tissue regeneration is lack of bioactive

recognition sites for cell adhesion and attachment. Proliferation of cells encapsulated in inert PEG hydrogel is quite limited [65]. Therefore, many studies have been done to chemically or physically incorporate bioactive motifs into PEG hydrogel network in order to enhance cell adhesion [60]. For example, various cell adhesion proteins including fibronectin, collagen, vitronectin, and laminin were chemically linked within hydrogel network using α-acryloyl-ω-N-hydroxysuccinimidyl ester PEG (Acryl-PEG-NHS) [66]. Peyton et al. conjugated oligopeptides in PEG hydrogel by homopolymerization of PEGDA with acrylated peptides [56]. However, this method required the functionalization of primary amine groups that may be a part of binding site and the modification process was quite complicated. Alternatively, bioactive motifs could be incorporated through a step-growth or mixed-mode thiol-acrylate reaction [46,67]. The peptides used in these cases have additional cysteine residues in the sequence. A fibronectin-derived peptide with the sequence Cys-Arg-Gly-Asp was routinely immobilized in PEG hydrogel network to improve cell attachment and adhesion [46]. PEG hydrogels with cell adhesion epitopes usually enhance cell viability and also stimulate cell proliferation [60].

1.2 Photopolymerization

Photopolymerization is an attractive method to form hydrogels via chemical crosslinking. The reason why photopolymerization has been investigated for a number of biomedical applications is that it can form materials in situ in a minimally invasive manner. Photopolymerization has several advantages over traditional polymerization techniques, including spatial and temporal control, fast gelation rate, and minimal heat production [68]. Photopolymerization process can be carried out under mild environment (e.g. room temperature, physiological pH solution) in the present of living cells.

1.2.1 Photoinitiation

Photoinitiation is the first step during photopolymerization. Photoinitiators, which have high absorption at specific wavelength of light, produce initiating radical species to trigger polymerization. Photoinitiator molecules absorb light in either ultraviolet (200-400 nm) or visible light (400-800 nm) range. There are typically two mechanisms to generate free radicals after light absorption [69]. One mechanism is that type I or cleavage-type photoinitiator cleaves directly into primary radicals. The other mechanism is that type II photoinitiator reacts with second species and abstracts hydrogen to form secondary radials [68]. For example, 2,2-dimethoxy-1,2-di(phenyl)ethanone (Irgacure 651), 2-hydroxy-1-[4-(2-hydroxyethoxy) phenyl]-2-methyl-1-propanone (Irgacure 2959, Figure 1.4(a)) and lithium phenyl-2,4,6-trimethyl-benzoylphosphinate (LAP, Figure 1.4(b)) are type I photoinitiators and cleave into two free radicals under UV light exposure. Camphorquinone and eosin Y (Figure 1.4(c)) are visible light photoinitiators and they both require co-initiator molecules to form free radicals. Camophorquinone is usually used with a hydrogen donating amine, while eosinY has been used in conjunction with triethanolamine (TEA, Figure 1.4(d)) [70].

Considering biocompatibility, only a few photoinitiators are suitable for biomedical applications. Irgacure 2959 was once a commonly used photoinitiator [72]. However, its solubility in water is quite low, less than 2 wt%. For cell encapsulation, lower wavelength light is not safe because it has potential to cause cell damage or mutation [73, 74]. The molar absorption coefficient (ε) of Irgacure 2959 at 365 nm is very low, approximately 10 $M^{-1}cm^{-1}$ [75]. Therefore, using Irgacure 2959 to initiate photopolymerization at higher wavelength is impossible. LAP, another type I photoinitiator, has been extensively used in many photopolymerization systems [43, 71], since Majima et al. [76] first synthesized it. Although the water-solubility of LAP is higher than Irgacure 2595 (up to 8.5 $wt\%$) and it enables cell encapsulation at lower initiator concentrations, LAP's utility in visible light range is still limited ($\varepsilon \approx 30$

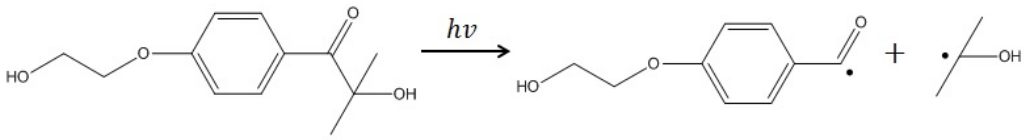

(a) Cleavage of I2959 into primary radicals following photon absorption

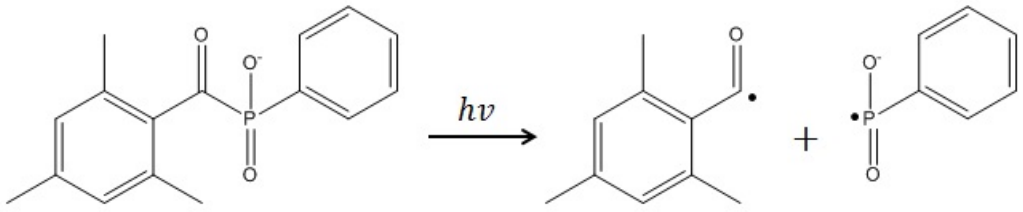

(b) Cleavage of LAP into primary radicals following photon absorption

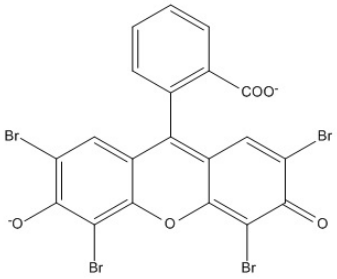

(c) EosinY

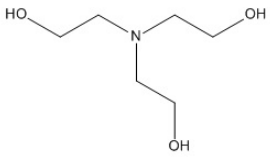

(d) TEA

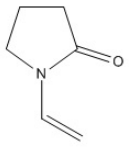

(e) NVP

Fig. 1.4. Photo-cleavable Type I photoinitiators: (a) I2959 and (b) LAP. Type II photoinitiator (c) eosinY requires co-initiator triethnonlamine (TEA) and co-monomer 1-vinyl-2-pyrrolidinone (NVP) to initiate photopolymerization [70, 71].

$M^{-1}cm^{-1}$ at 405 nm) [77]. Compared with Irgacure 2959 and LAP, type II photoinitiator eosin-Y is a perfect candidate because it is highly water-soluble (400 g/l) and absorbs light at visible light range ($\varepsilon \approx$ 100,000 $M^{-1}cm^{-1}$ at 516 nm) [28, 78]. For example, Bahney et al. [79] have produced PEG-acrylate hydrogels using eosinY as initiator via visible-light mediated photopolymerization. However, as a type II initiator, eosinY requires co-initiator (triethnonlamine, TEA) to generate radicals and co-monomer (1-vinyl-2 pyrrolidinone, NVP, Figurer 1.4(e)) to facilitate hydrogel gelation. The concentration of TEA in conventional visible-mediated photopolymer-

ization is approximately 200 mM, which cause undesired cytotoxic effect to some sensitive cell types [44].

1.2.2 Chain Growth, Step Growth and Mixed-mode Polymerization

In the formation of typical chain-growth network (Figure 1.5(a)), free radicals rapidly propagate through carbon-carbon double bonds on the monomers or macromers to form the high-molecular-weight kinetic chains by covalently crosslinking. For example, PEG-diacrylate can form purely chain-growth hydrogel using eosinY as initiator, TEA as co-initiator and NVP as co-monomer in previous study [79]. Incorporating hydrolytically cleavable ester groups [60] or enzymatically cleavable peptides [80] can regulate degradation of chain-growth network. However, hydrogels via chain-growth polymerization have some limitations for biomedical applications. First, high-molecular-weight kinetic chains cannot be degraded [81]. Second, chain-growth polymerization usually has a low conversion of functional groups. The remaining unreacted monomers can be cytotoxic, causing local inflammatory response in the body [82]. Finally, hydrogels formed via chain-growth have heterogeneous network [83], which may affect drug release performance when utilized in pharmaceutical application.

As an alternative to form hydrogels *in situ*, many studies have been done to develop degradable networks formed via Michael addition reaction (Figure 1.5(b)), which is a type of step-growth polymerization, between thiol and acrylate [40], maleimide [41] or vinylsulfone functional groups [42]. In this step-growth polymerization, a reactive thiolate ion reacts with a vinyl functional group to form a carbon-based anion, which then reacts with another thiol group to regenerate another thiolate ion. The repetition of these events leads to the formation of covalently crosslinked hydrogel [61]. Compared with chain-growth structure, such network has several advantages: 1) high molecular weight kinetic chains are not produced; 2) it can form more homogenous structure with better control of crosslinking density and material properties, which

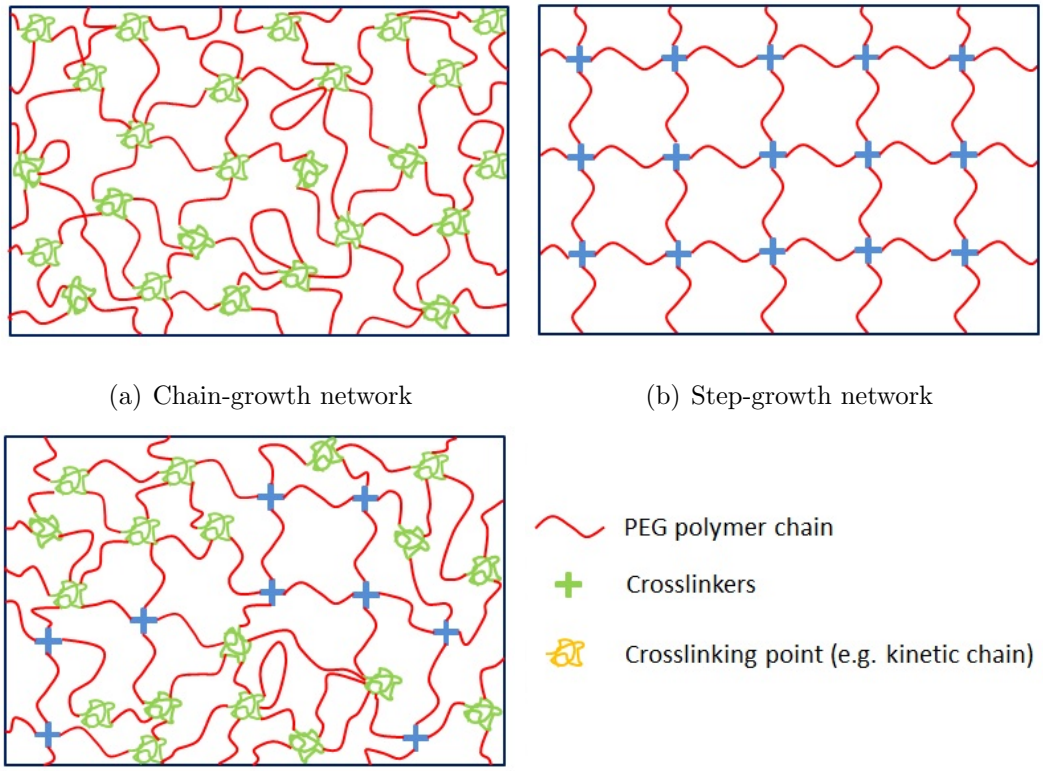

(a) Chain-growth network

(b) Step-growth network

(c) Mixed-mode network

Fig. 1.5. Schematic structures of PEG hydrogels formed through (a) chain-growth, (b) step-growth, and (c) mixed-mode step-and-chain-growth polymerization [23]

is quite important in application for drug delivery [51] and 3) it does not need any initiator and can be catalyzed in a mildly basic environment. However, Michael type addition reaction does not possess spatially and temporally control over the network formation, and its gelation rate is much slower compared with chain-growth polymerization.

Mixed-mode photopolymerization (Figure 1.5(c)) is the combination of both chain and step growth reactions. The free radical propagation mechanism is showed in the Figure 1.6. First, thiyl radical reacts with vinyl functional group to form a carbon-based radical, which then can get involved into two different pathways. One is that carbon-based radical reacts with another thiol group to regenerate thiyl radical. This

is similar to step-growth polymerization in which the propagation of free radicals and chain transfer occur sequentially. The other pathway is the carbon-based radical reacts with another vinyl-based monomer or macromer, which is same as chain-growth polymerization where free radicals propagate along the double bonds [45, 46]. Hydrogels fabricated via this mixed-mode polymerization possess a less heterogeneous network compared with those formed through purely chain-growth reaction. The gelation rate of mixed-mode photopolymerization is much faster than that of Michael type step-growth reaction. Besides all of these merits, thiol-vinyl network has a unique and important property. Its structure is directly impacted by the thiol:vinyl ratio. As thiol-to-vinyl ratio increases, network transfers from chain-growth-like structure to more step-growth-like structure. In addition, other properties, such as swelling, stiffness and degradation, can also be tuned by changing the thiol-to-vinyl ratio [61]. For example, when thiol-to-vinyl ratio increases, degradation rate of thiol-vinyl hydrogel becomes faster because more thiol-ester bonds forming when increasing the concentration of thiol functional groups.

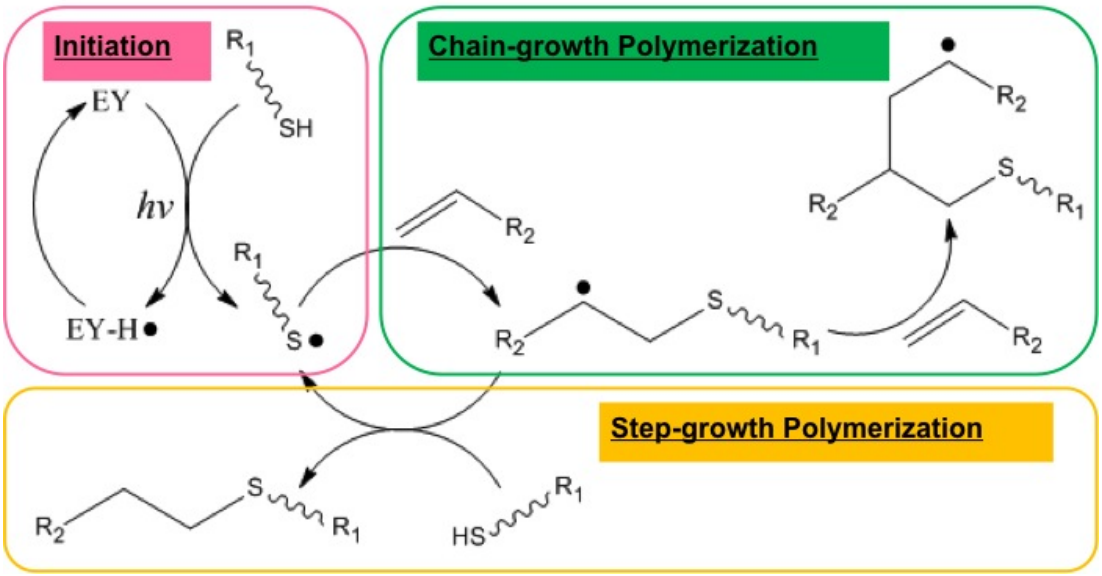

Fig. 1.6. Sequential Addition and Hydrogen Abstraction Steps during a Thiol-acrylate Polymerization

2. OBJECTIVES

2.1 Evaluate the Possibility of Using Thiol-containing Molecules to Replace TEA

Conventional visible light-mediated photopolymerization requires use of co-initiator TEA at high concentration ($\approx 200\ mM$), which is cytotoxic and therefore restricts its applications in biomedical fields. Here, TEA was replaced by thiol containing molecules. During photoinitiation, excited eosinY reacts with thiol containing molecules and abstracts hydrogen to form thiyl radicals, which can then crosslink with acrylate. So thiol containing molecules act as both co-initiator to regenerate free radicals and crosslinker to form hydrogel network. In this thesis, fabrication of PEG-diacrylate hydrogels was first developed using thiol-containing molecules instead of TEA via mixed-mode polymerization. Co-monomer NVP was used in this process to facilitate gelation process. In addition, factors that affect properties of PEG-diacrylate hydrogels were also investigated. These factors include concentration of eosinY, polymerization time, molecular weight of PEGDA macromer, thiol content, NVP concentration, and ratio of thiol-to-acrylate. Furthermore, bioactive RGDS motifs were incorporated into hydrogels via two different methods to enhance cell attachment and adhesion. The incorporation efficiency of pendant peptide RGDS and their effects on gel properties were also investigated.

2.2 Utilize PEG-tetra-acrylate to Form Hydrogels via the Same Mixed-mode Mechanism

To form PEGDA hydrogel via this mixed-mode photopolymerization required high concentration of macromer (more than 10 $wt.\%$). Since hydrogels are only formed

when the ratio of thiol-to-acrylate in a certain range, high concentration of acrylate means high consumption of thiol containing molecules. Therefore, fabrication of hydrogel using PEG-tetra-acrylate (PEG4A) was conducted. Since PEG4A has four vinyl functional groups, it should form tight crosslinked network at low macromer concentration. The factors that can affect PEG4A hydrogels properties, such as concentration of NVP and thiol, were also investigated.

3. MATERIALS AND METHODS

3.1 Materials

PEG-diacrylate, 4-arm PEG-hydroxyl and 4-arm PEG-amine were obtained from JenKem Technology USA. Triethanolamine (TEA), and N-vinylpyrrolidone (NVP) were purchased from Alfa Aesar and Acros Organics, respectively. Eosin-Y disodium salt was obtained from MP Biomedical. Dithiothretiol (DTT) was purchased from Thermo Fisher. Fmoc-amino acids and peptide synthesis reagents were purchased from Chempep or Anaspec. HPLC grade acetonitrile and water were acquired from Thermo Fisher and VWR international, respectively. All other chemicals were acquired from Sigma-Aldrich unless otherwise noted.

3.2 Synthesis of PEG Macromers

PEG-diacrylate (PEGDA), PEG-tetra-acrylate (PEG4A) and PEG-tetra-acrylamide (PEG4AA) were synthesized using 4-arm PEG-hydroxyl (PEG-OH) or 4-arm PEG-amine (PEG-NH_2). Prior to reaction, PEG-OH or PEG-NH_2 was dried azeotropically in anhydrous toluene. Then acryloyl chloride (8 eq. of OH or NH_2 group on PEG) and triethylamine (8 eq.) dissolved in anhydrous toluene were added slowly to the PEG/toluene solution through an addition funnel. The reaction was allowed to proceed overnight at room temperature in the dark. Next, the solution was filtered through neutral aluminum oxide to remove triethylamine salt and stirred for 2 h with sodium carbonate. The heterogeneous solution was filtered through a thin layer of Hyflo, followed by precipitation in cold ethyl ether.

PEG-tetra-methacrylate (PEG4MA) was synthesized by a microwave-assisted reaction. Briefly, 4-arm PEG-OH was added to 8 eq. of methacrylic anhydride in a

round bottom flask. The flask was placed in the microwave-assisted reactor (CEM Discover SPS) and the reaction proceeded at a microwave power of 300 W and 60°C for 5 min. The product was precipitated in cold ethyl ether and collected via filtration.

PEG-tetra-allylether (PEG4AE) was synthesized as described previously. First, sodium hydride (NaH, 1 eq.) was added slowly into a flask containing dried 4-arm PEG-OH dissolved in anhydrous tetrahydrofuran (THF). After the release of hydrogen gas, allyl bromide (6 eq. of OH group) was added into the flask slowly and the reaction was kept at 40°C for overnight. The product was filtered and precipitated in cold ether. All PEG macromers were characterized by H^1NMR (AVANCE Bruker 500) and stored at -20°C until use. The degrees of functionalization for all PEG macromers were at least 95%.

3.3 Peptide Synthesis and Purification

All peptides were synthesized using solid phase peptide synthesis in a microwave peptide synthesizer (CEM Discover SPS). Briefly, Fmoc-Rink Amide MBHA resin was swell in dimethylformamide (DMF) for 15 min. The deprotection procedures (in 20% piperidine in DMF with 0.1 M HOBt) were performed in the peptide synthesizer for 3 min at 75°C with microwave power set at 50 W. Fmoc-protected amino acids were dissolve in 8mL activator solution (0.28 M Diisopropylethylamine in DMF) before coupling. The activated Fmoc-amino acid solution was added to the deprotected resin and the coupling reactions were performed in the synthesizer for 5min at 75°C and 50 W. For coupling with Cystein and Histidine amino acids, the reactions were performed for 10min at 50°C and 50 W. Ninhydrin test was conducted after each deprotection and coupling step. The synthezised peptides were cleaved in 5 mL cleavage cocktail (250 mg phenol, 4.75 mL Trifluoroacetic acid, 0.125 mL trisopropylsilane and 0.125 mL distilled water) for 30 min at 38°C and 20 W. Cleaved peptides were precipitated in cold ether for three times, dried in vacuo and stored in -20°C.

After synthesis, all peptides were purified to at least 90% pure by reverse phase high-performance liquid chromatography (HPLC, Perkinelmer Flaxer).

3.4 Hydrogel Fabrication

Mixed-mode thiol-vinyl hydrogels were formed by visible light mediated polymerization between PEG macromer (PEGDA, PEG4A, PEG4AA, PEG4MA, or PEG4AE) and di-thiol containing cross-linker (DTT or bis-cysteine containing peptides), which were dissolved in pH 7.4 phosphate buffered solution (PBS). Eosin-Y and N-vinylpyrrolidone (NVP) were added to the precursor solution, which was injected between two glass slides separating by two 1mm Teflon spacers and then exposed under visible light at 70,000 Lux. In some controlled experiments, TEA was used as a co-initiator to yield purely chain-growth non-degradable PEGDA hydrogels.

3.5 Gel Swelling

For gel swelling studies, each gel was prepared from 50 μL of precursor solution following the gelation procedure described above. After gelation, samples were incubated in pH 7.4 PBS at 37°C on an orbital shaker for 24 h. Gels were then removed from the buffer and weighed to obtain swollen weights ($W_{swollen}$), followed by drying in vacuuo for 24 h to obtain dried polymer weights (W_{dry}). Hydrogel mass swelling ratio (q) was defined as $W_{swollen}/W_{dry}$. Hydrogel degradation was monitored by changes in hydrogel shear modulus as time. Hydrogel shear modulus is positively correlated to the gel crosslinking density, which decreases exponentially as time for hydrolytic bulk gel degradation.

3.6 Gel Fraction

To test gel fraction, each gel was prepared from 25 μL of precursor solution within syringe. After gelation, samples were dried in vacuo to get the first dried weight

(W_{dry1}). Then each gel was placed in pH 7.4 PBS at 37°C on an orbital shaker for 24 h. After one day swelling, samples were dried again in vacuo to get the second dried weight (W_{dry2}). The gel fraction can be obtained via this equation:

$$Gel fraction = \frac{W_{dry2}}{W_{dry1}} \tag{3.1}$$

This parameter can reflect the percentage of macromer that crosslinked into hydrogels.

3.7 Real-time Rheometry

Real-time photorheometry was used to determine gel points (i.e., cross-over time). Briefly, macromer solution was placed in the light cure cell in Bohlin CVO 100 digital rheometer. The sample was irradiated with visible light (halogen cold light lamp from AmScope, Inc., 70,000 Lux) through a flexible light guide. Time-sweep measurements were operated at 10% strain, 1Hz frequency, 0.1 N normal force, and 100 μm gap size. The storage (G') and loss (G'') moduli were recorded in the linear viscoelastic region and gel points were identified by the time at which G' surpassed G''.

3.8 Degradation Test

The degradation behavior of hydrogels was observed by tracking the change of storage moduli. For rheometrical property measurements, hydrogels were fabricated between two glass slides with 1 mm thick spacers and then were punched into circular gel discs (8 mm in diameter) using a biopsy punch. Punched gel discs were placed in PBS with pH 7.4 and were measured at certain time intervals. Strain-sweep (0.1% to 5%) oscillatory rheometry was performed, on a Bohlin CVO 100 digital rheometer, to measure gel moduli using parallel plate geometry (8 mm) with a gap size of 750 μm.

3.9 Peptide Incorporation Efficiency

The incorporation efficiency of pendant peptide (Ac-CRGDS or Acryl-RGDS. Underlines indicate cross-linkable moieties) in the hydrogel was characterized by analytical RP-HPLC. In addition to the macromer and initiator components, peptide Ac-CRGDS (Figure 3.1(a)) or Acryl-RGDS (Figure 3.1(b)) was added in the pre-polymer solution at 1mM. Peptide-immobilized hydrogels (25 μl each gel) were prepared via the same visible light exposure as described above. After gelation, samples were incubated in 200 μl ddH_2O in microtubes kept at 37°C on an orbital shaker for 1 to 4 days. The solutions were then removed from microtubes and subjected to analytical RP-HPLC to determine the concentration of the released peptide. A series of peptide solutions with known concentrations were analyzed to generate standard curves, which were used to determine the concentration of the released peptide. Peptide incorporation efficiency was determined by mass balance calculation.

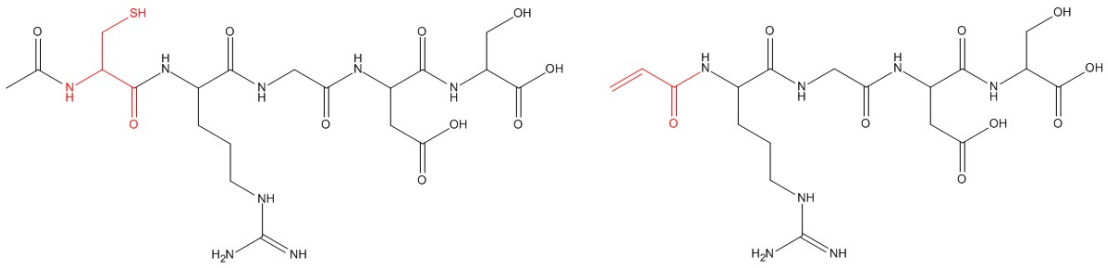

(a) Acetylated-CRGDS (b) Acrylated-RGDS

Fig. 3.1. Chemical structures of pendant peptides. Red labeled structures indicate cross-linkable moieties.

4. RESULTS AND DISCUSSION

4.1 Develop a Visible Light-Mediated Thiol-acrylate Photopolymerization

As mentioned in the Section 1.2.2, there are disadvantages to fabricate hydrogels via purely chain-growth photopolymerization or Michael addition reaction. In this thesis, formation of visible light-mediated hydrogels via mixed-mode polymerization was investigated. The mechanism involved has been demonstrated in Section 1.2.2 and showed in Figure 1.6. Briefly, eosinY becomes excited after absorbing photons from visible light and abstracts one hydrogen from thiol to form a thiyl radical. Thiyl radicals react with acrylate functional groups in PEG macromer to generate carbon-based radicals. Carbon-based radicals can either homopolymerize with acrylates or react with thiol to regenerate thiyl radicals. The macromer used here was PEG-diacrylate (PEGDA), which had two acrylate functional groups. Dithiothreitol (DTT) was used to replace co-initiator TEA in conventional visible light-mediated photopolymerization and functioned as both co-initiator and crosslinkers. The photoinitiator was eosinY, which had high absorption at visible light range. 1-vinyl-2 pyrrolidinone (NVP) was added as co-monomer to accelerate gelation process.

First, the possibility of using thiol-containing molecules to replace TEA was evaluated. PEGDA with molecular weights of 2, 3.4 or 10 kDa and concentrations of 10 or 15 $wt.\%$ were used. According to the results (Figure 4.1), there was parabolic relationship between thiol concentration in precursor solution and elastic modulus of resulting hydrogels for all groups with different molecular weights. In other word, in each group with the same molecular weight and macromer concentration, the elastic modulus increased first and then started to drop as the increase of thiol concentration. Furthermore, as the molecular weight of PEGDA decreased, more bi-functional

thiols were needed to reach maximum gel modulus. For example, when 10 $wt.\%$ $10kDa$ PEGDA was used, the thiol concentration required to form hydrogel with highest elastic modulus was 5 mM (corresponding to 2.5 mM DTT); while when using 10 $wt.\%$ 3.4 or $2kDa$ PEGDA, bi-functional thiol concentration increased to 20 mM or 60 mM respectively (Table 4.1). In addition, increasing the concentration of PEGDA macromer from 10 $wt.\%$ (Figure 4.1(a)) to 15 $wt.\%$ (Figure 4.1(b)) increased the overall hydrogel stiffness. For example, the highest elastic modulus for the group using 10 $wt.\%$ $3.4kDa$ PEGDA was about $4.6kPa$, while it increased to approximately $11.2kPa$ when using 15 $wt.\%$. Moreover, increasing macromer concentration also broadened the range of bi-functional thiol concentrations necessary for forming hydrogel.

Table 4.1.
Formulations of visible light curable PEGDA hydrogels with DTT as co-initiator and crosslinker.

PEGDA ($wt.\%$)	PEGDA m.w. (Da)	Acrylate (mM)	$[SH]_{DTT}$ $(mM)^a$	[SH]/[acrylate]	[SH]/[vinyl]^b
10	2,000	100	20-80	0.2-0.8	0.183-0.734
	3,350	60	5-40	0.08-0.67	0.072-0.580
	10,000	20	2.5-10	0.13 -0.5	0.086-0.345
15	2,000	150	20-150	0.13-1	0.126-0.943
	3,350	90	5-90	0.06-1	0.051-0.909
	10,000	30	2.5-20	0.08-0.67	0.064-0.513

$^a[SH]_{DTT}$ represents thiol concentration, which is twice the concentration of DTT.

^{b}[vinyl] = [acrylate] + [NVP]. All precursor solutions contain 9.4 mM (0.1 $vol.\%$) NVP.

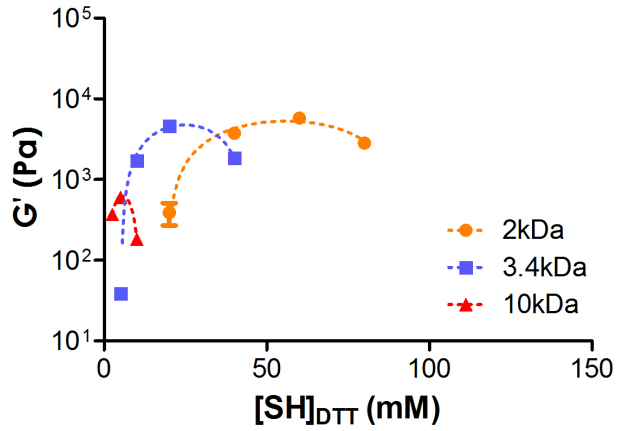

(a)

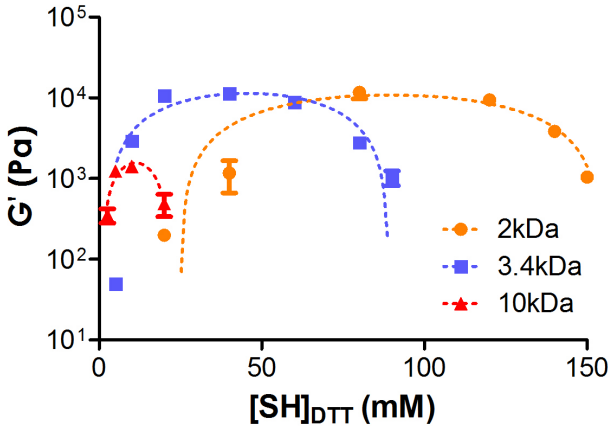

(b)

Fig. 4.1. Effect of PEGDA molecular weight and bi-functional thiol concentration on equilibrium elastic modulus measured at day-1 post gelation. $3.4kDa$ PEGDA macromers were used at: (a) 10 wt.% and (b) 15 wt.%. All hydrogels were prepared with 0.1 mM eosinY and 0.1% NVP and with 5 min of visible light exposure. Non-linear curve fitting was conducted using parabolic relationships as a function of thiol concentration.

Unlike co-initiator TEA in conventional visible light mediated gelation, thiol containing molecules (e.g., DTT) have multiple roles. In the mixed-mode scheme as stated before, DTT is not only a co-initiator that provides thiyl radical for photoinitiation, but also a linker and chain-transfer agent that impacts the degree of gel crosslinking. According to data showed in the Figure 4.1 and the Table 4.1, highly cross-linked hydrogels could only be formed when thiol-to-acrylate ratio was in a certain range. Initial increase of thiol content in the precursor solution increased gel elastic modulus, which was due to the increasing concentration of thiyl radicals that accelerated gelation kinetics. However, further increasing of thiol content led to decrease of gel stiffness. This was because more thiol increased the chance of chain-transfer events and decreased the degree of homopolymerization. Therefore, more acrylates participated in step-growth polymerization, rather than chain-growth. PEGDA and DTT all have two functional groups, which means they form linear structure when undergoing step-growth polymerization. Such linear structure can not make contribution to gel stiffness. Theoretically, when ratio of thiol-to-acrylate equals to one, it would result in the linear structure, not cross-linked network. However, in the experiment, hydrogels could be fabricated at a unity thiol-to-acrylate ratio. This is because using 0.1 $vol\%$ NVP decreases total thiol-to-vinyl ratio (Table 4.1). The effect of NVP will be discussed later.

4.2 Investigate Factors Affecting the Properties of PEG-diacrylate Hydrogels

According to the previous results, PEGDA hydrogels can be fabricated via visible light-mediated mixed-mode polymerization. In the next chapter, methods to regulate gel properties, including gel stiffness, degradation rate, and gelation rate etc., were investigated.

4.2.1 Effect of EosinY Concentration on Gel Properties

Changing eosinY concentration can affect hydrogel properties, such as gelation rate, elastic modulus, swelling, and degradation. Figure 4.3(a) shows the influence of eosinY concentration on gelation kinetics. *In situ* photorheometry was conducted for hydrogels prepared from 10 $wt.\%$ 3.4kDa PEGDA, 10 mM DTT, 0.1% NVP with different concentration of eosinY (0.025, 0.05 or 0.1 mM). Gel points decreased from 249±14 sec to 156±3 and 125±11 sec as the concentration of eosinY increased. Figure 4.3(b) shows the results of gel stiffness when using different eosinY concentration. The direction of arrow in this figure indicates the increase of eosinY content. According to the Figure 4.3(b), hydrogels possess higher elastic modulus with higher eosinY concentration in precursor solution, $G' \sim 0.4$, 1.4, and 1,8 kPa for gels formed with 0.025, 0.05 and 0.1 mM eosinY respectively. The swelling property of hydrogels also indicates the improvement in gel crosslinking at higher eosinY content. Figure 4.3(c) shows the equilibrium mass-swelling ratio Q_m decreases as increasing of eosinY concentration.

In addition, Figure 4.4 shows the effect of eosinY concentration on hydrogels degradation property. Thiol-acrylate hydrogels are hydrolytically degradable due to the formation of thiol-ester bonds in the network (Figure 4.2).

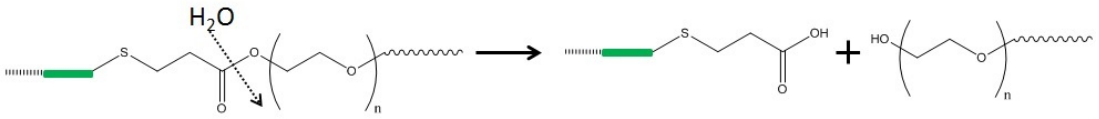

Fig. 4.2. Hydrolysis of thiol-ether-ester bond

Such hydrogel undergoes bulk degradation, which means degradation occurs throughout the whole material equally. As mentioned before in the Section 1.1.4, elastic modulus G' of hydrogels, which follow bulk degradation, should decrease exponentially as function of time.

$$\frac{G'}{G'_0} = e^{-kt} \tag{4.1}$$

and

$$\ln \frac{G'}{G'_0} = -kt \tag{4.2}$$

where G'_0 is the initial elastic modulus and k is pseudo-first order degradation rate constant.

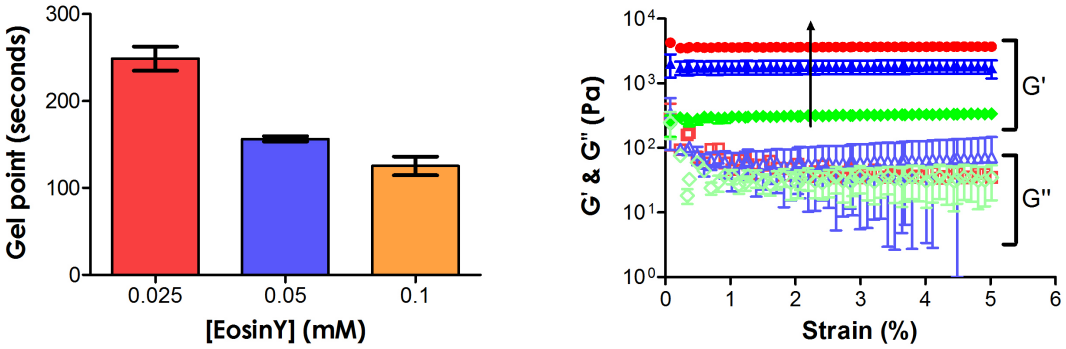

(a)

(b)

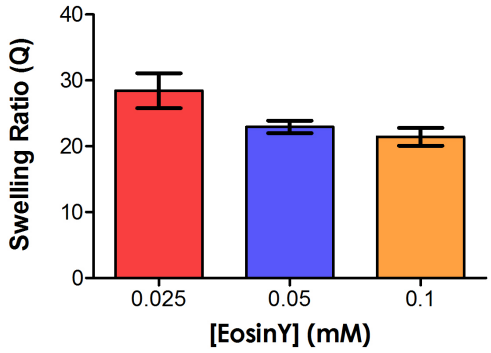

(c)

Fig. 4.3. Physical properties of visible light cured PEGDA thiol-acrylate hydrogels formed with 0.025, 0.05, or 0.1 mM of eosinY. (a) Gel points; (b) Elastic (G') and viscous (G'') modulus and (c) Equilibrium mass swelling Ratio (Q). All properties were measured at day-1 post gelation. Hydrogels were prepared from 10wt.% 3.4kDa PEGDA with 10mM DTT and 0.1%NVP, and with 5 min visible light exposure.

In the Figure 4.4(a), elastic modulus of hydrogels were plotted as a function of degradation time. Since the y-axis is on log scale, the slopes of the exponential fitting curves represent degradation rate constants (k_{hyd}). The larger the k_{hyd} is, the faster the degradation is. This is the method to evaluate degradation rate. Figure 4.4(b) shows the linear relationship between eosinY concentration and degradation rate constant. As expected, with higher concentration of eosinY, hydrogels undergo slower degradation. Increasing eosinY concentration leads to generation of more free radicals, which can accelerate gelation process. Therefore, a higher crosslinked network forms with higher modulus, smaller swelling ratio, and slower degradation rate.

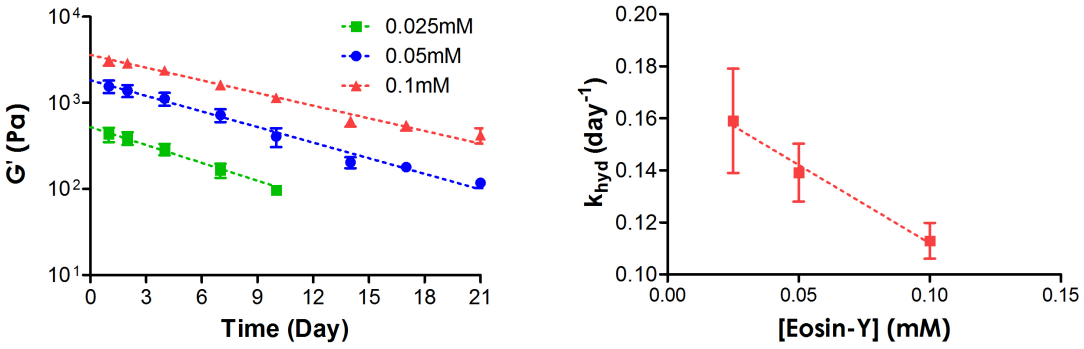

(a) (b)

Fig. 4.4. Effect of eosinY concentration on gel degradation. (a) Hydrogel elastic modulus were plotted as a function of degradation time. All gels were prepared from 10wt.% 3.4kDa PEGDA with 10mM DTT and 0.1%NVP, and with 5 min visible light exposure. Gel degradation was conducted in pH 7.4 PBS at 37°C. (b) Hydrolytic degradation rate constants (k_{hyd}) obtained from (a) and plotted as a function of eosinY concentration. Curves indicate an empirical fitting with a linear relationship ($N = 3, Mean \pm SD$)

4.2.2 Effect of Thiol Concentration on Hydrolytic Degradation of PEGDA Hydrogels

As mentioned in the Section 1.1.4, mixed-mode thiol-acrylate hydrogels are degradable because of the formation of thiol-ester bonds, which are susceptible to hydrolytic degradation. Changing the thiol concentration in the precursor solution could affect thiol-ester bond formation and therefore regulate degradation rate of PEGDA hydrogels. Figure 4.5 shows the effect of thiol concentration on hydrolytic degradation. All hydrogels were prepared from 10 $wt.\%$ $3.4kDa$ PEGDA with 0.1 mM eosinY. NVP was added at 0.0% (Figure 4.5(a)), 0.1% (Figure 4.5(b)) and 1.0% (Figure 4.5(c)). Various concentrations of bi-functional thiol from DTT were used from lowest 7.5 mM to highest 45 mM. Increasing of NVP concentration resulted stiffer hydrogels with slower degradation rate. In the Figure 4.5(a), all PEGDA hydrogels without NVP degraded very fast and completely dissolved in one week. When using 0.1 $vol\%$ NVP (Figure 4.5(b)), most hydrogels weaken as time, but remained intact after three weeks, except groups with 40 mM and 45 mM thiols. Hydrogels with 1.0% NVP were much more stable and all can last for three weeks (Figure 4.5(c)). More details about the effect of NVP concentration on hydrogel properties will be discussed in later section.

Table 4.2.
Exponential curve fitting of hydrogel degradation rate constant (k_{hyd}) as a function of bi-functional thiol concentration at different NVP contents. All analysis were based on the data in the Figure 4.5(d).

NVP ($vol\%$)	Slope	R^2
0	0.034±0.007	0.92
0.1	0.049±0.003	0.99
1.0	0.071±0.006	0.98

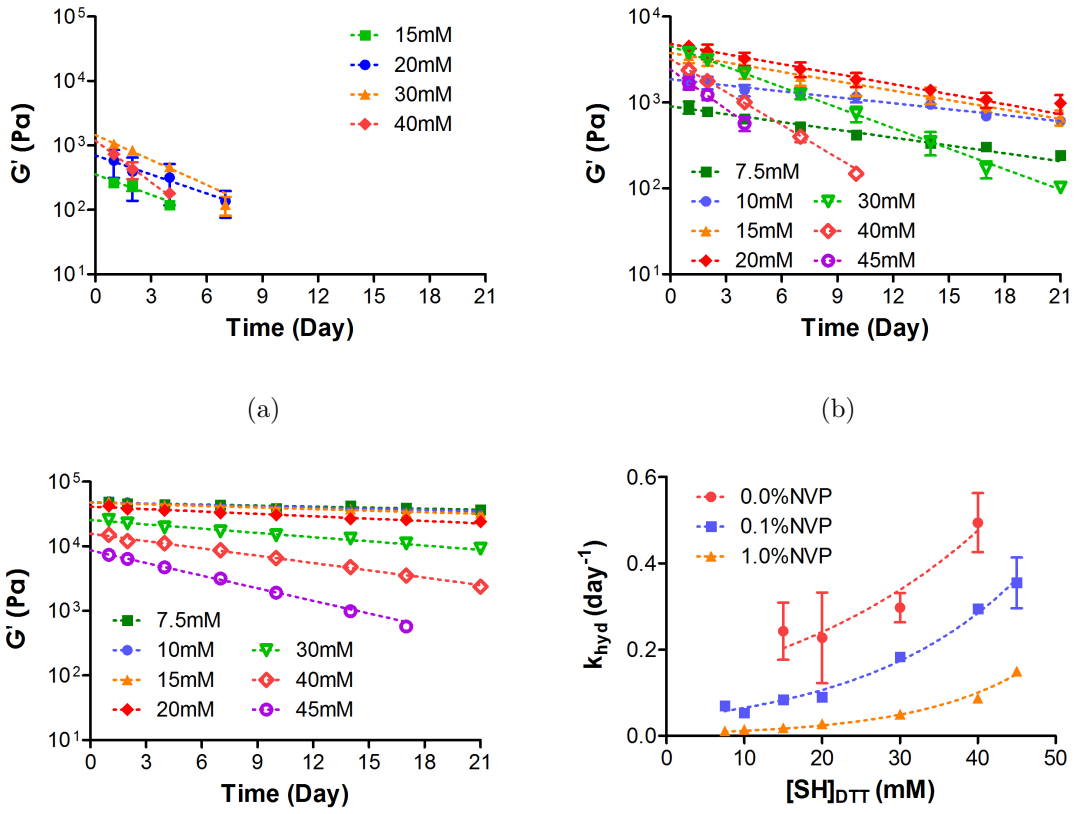

Fig. 4.5. Effect of thiol concentration on hydrolytic degradation of mixed-mode PEGDA hydrogels. All gels were prepared from 10wt.% 3.4kDa PEGDA with 0.1 mM eosinY. NVP was added at: (a) 0%, (b) 0.1% and (c) 1.0%. All degradation profiles were conducted using exponential curve fitting (log scale on Y-axis). (d) Hydrolytic degradation rate constants (k_{hyd}) obtained from (a-c) and plotted as a function of thiol concentration with an exponential growth fitting ($N = 3, Mean \pm SD$).

Degradation rate constant (k_{hyd}) were obtained from the data in the Figure 4.5(a)-(c). To reveal the relationship between k_{hyd} and thiol concentration, k_{hyd} was plotted as function of thiol concentration in the Figure 4.5(d). Obviously, k_{hyd} decreases as increasing of NVP content for all thiol concentrations. Furthermore, the value k_{hyd} increases exponentially as a function of thiol concentration (Tabel 4.2). Although the mechanism behind this exponential relationship is not clear, it still could serve as a method to predict hydrogel degradation property.

4.2.3 Effect of Polymerization Time on Gel Degradation

Changing polymerization time is also another method to regulate gel degradation property. Exposure of eosinY to light for longer time could generate more free radicals for mixed-mode potopolymerization. Figure 4.6 shows the effect of polymerization time on gel degradation behavior. All PEGDA hydrogels were fabricated using 10 $wt.\%$ $3.4kDa$ PEGDA, 0.1 mM eosinY, and 0.1% NVP. Various thiol concentrations were used from 7.5 mM to 45 mM. According to the Figure 4.6(b), degradation rate constant (k_{hyd}) decreased as photopolymerization time increased at all thiol concentrations.

4.2.4 Effect of Pendant Peptide on Gel Properties

As mentioned in the Section 1.1.5, immobilization of bioactive motifs is necessary to improve cell adhesion and attachment when designing hydrogels for cell encapsulation. Here the influences of incorporated pendant peptide on hydrogel properties were investigated (Figure 4.7).

Hydrogels were prepared from 10 $wt.\%$ $3.4kDa$ PEGDA, 0.1 mM eosinY and 0.1% NVP at various thiol concentrations. Incorporated peptide was either 1 mM of acetylated-CRGDS (Ac-CRGDS) or 1 mM of acrylated-RGDS (Acryl-RGDS). Hydrogels without pendant peptides (blank) was tested as a control group. These two peptides were incorporated into hydrogel via different reactions. Acrylated-RGDS was

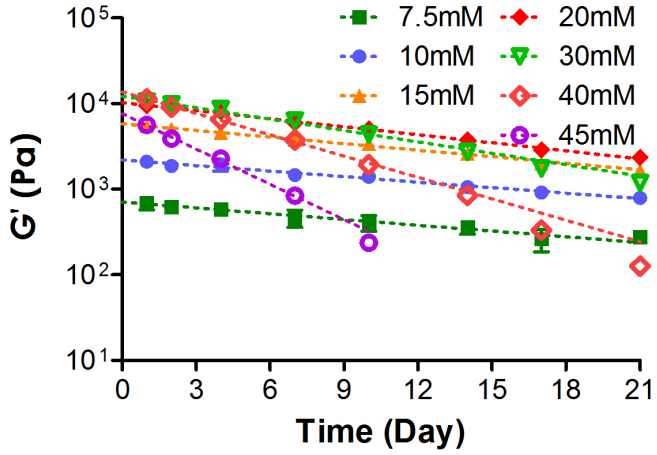

(a)

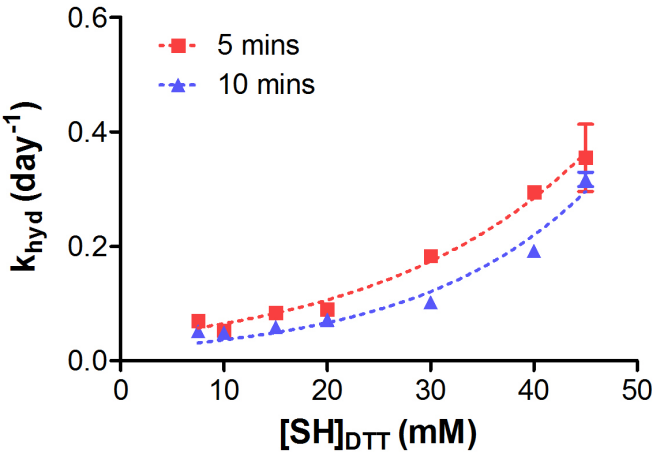

(b)

Fig. 4.6. Effect of time polymerization time on gel degradation. Hydrogels were prepared by 10 wt.% 3,4kDa PEGDA, 0.1mM eosin-Y and 0.1% NVP. The polymerization time was 5 min showed in Figure 4.5(b) or (a) 10 min. Gel degradation was conducted in pH 7.4 PBS at 37°C. (b) Hydrolytic degradation rate constants (k_{hyd}) obtained from Figure 4.5(b) and (a). (k_{hyd}) was plotted as function of thiol concentration with an exponential growth fitting ($N = 3, Mean \pm SD$).

crosslinked into network through reaction with free radicals species, while acetylated-CRGDS was immobilized through step-growth thiol-to-acrylate reaction.

Figure 4.7(a) shows the influence of pendant peptides on hydrogel stiffness. The addition of pendant peptides decreases elastic modulus of hydrogels. Specifically, the incorporation with Acryl-RGDS resulted approximately 20-40% reduction of gel stiffness, while immobilization with Ac-CRGDS caused 30-60% reduction. This result is consistent with previous study, which has showed similar decrease in gel stiffness when acrylated peptides were crosslinked via a purely chain-growth photopolymerization with TEA [28]. Compared to the hydrogels with Acryl-RGDS, the incorporation of cysteine-containing peptide caused more reduction in gel stiffness. The reason why hydrogels with immobilization of Ac-CRGDS possess weaker mechanical property could be that the use of higher thiol pushed the network to adapt more "step-growth" structure with higher degree of thiol-acrylate chain transfer and lower degree of acrylate homopolymerization. Figure 4.7(b) shows the effect of pendant peptide on gel fraction. For all groups (blank, with Ac-CRGDS and with Acryl-RGDS), gel fraction increases as increasing thiol concentration. However, pendant peptides did not affect gel fraction so much when compared with hydrogels without peptide.

The incorporation efficiency of both pedant peptides were evaluated using RP-HPLC. Decent immobilization efficiency of peptides is important because unreacted soluble peptides can compete with immobilized peptides for cell receptors, which leads to less cell attachment to hydrogel network. Figure 4.7(c) shows the results of incorporation efficiency of Ac-CRGDS and Acryl-RGDS. The immobilization efficiency of Ac-CRGDS remained quite high (87%$\sim$90%) no matter what thiol concentration was used, while the incorporation efficiency of Acryl-RGDS was much lower (33%$\sim$67%) and was fluctuated when changing thiol concentration. Elbert et al. [31] have reported low immobilization efficiency (23%$\sim$66%) of acrylated-peptide in visible light curable purely chain-growth hydrogel, which is quite similar to the results here. Salinas and Anseth [46] have reported high peptide immobilization efficiency (85%$\sim$95%) in UV-mediated mixed-mode photoplymerization. Here our visible light-mediated

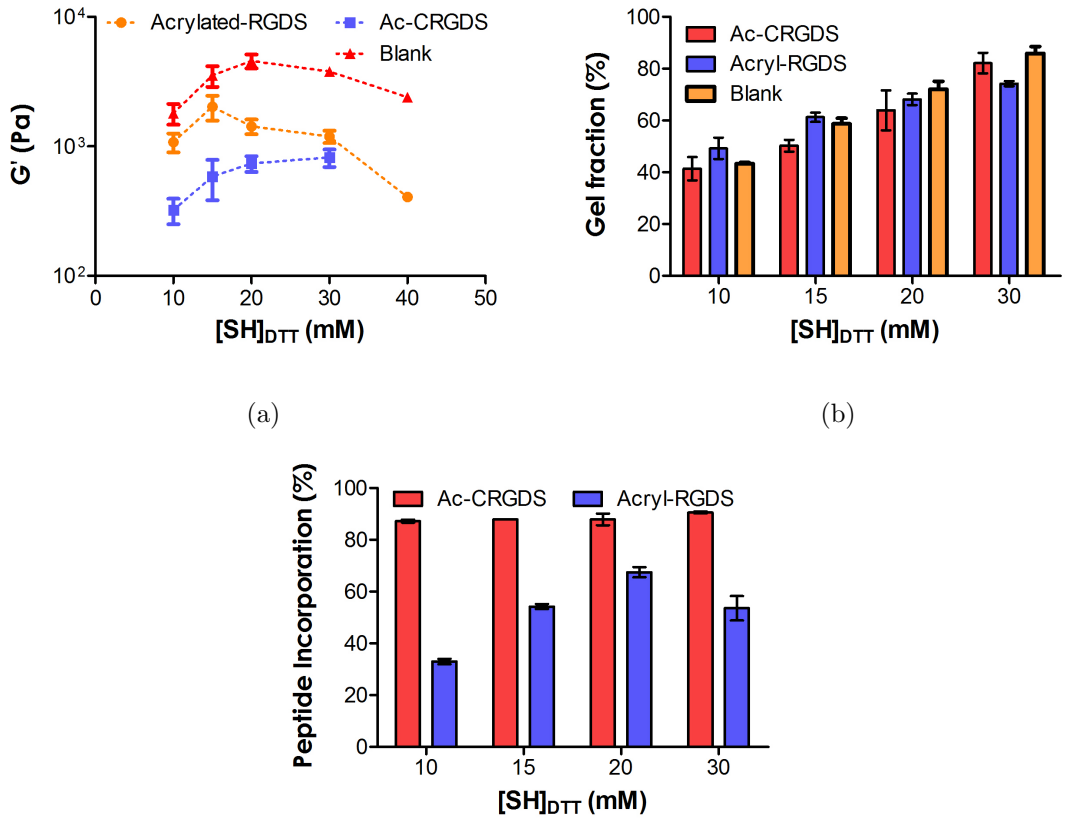

(a) (b)

(c)

Fig. 4.7. Effect of pendant peptide (i.e., Acryl-RGDS or Ac-CRGDS) and thiol content on: (a) Equilibrium elastic modulus (G'), measured at day-1 after gelation, (b) Gel fraction, (c) Mass swelling ratio (Q), also measured at day-1 post gelation and (d) Peptide immobilization efficiency. All hydrogels were prepared from 10 wt.% 3.4kDa PEGDA with 0.1 mM eosinY and 0.1% NVP and with 5 min of visible light exposure. All peptides were incorporated at 1 mM in the pre-polymer solutions. Gels without pendant peptide (i.e., Blank) were used as control for statistical analysis.

thiol-acrylate system also exhibits high degree of peptide immobilization. The reason why Ac-CRGDS has higher incorporation efficiency is that it can be crosslinked into network via Michael type addition even without photoinitiator.

Figure 4.8 shows the effect of pendant peptide on gel hydrolytic degradation. Hydrogels with 1 mM Ac-CRGDS or Acryl-RGDS degrade faster than those without incorporated peptide. As discussed before, the incorporation of pendant peptides negatively affected the stiffness of hydrogels, which indicated the decrease in crosslinking density. Hydrogels with lower crosslinking density exhibit faster degradation rate. This is the reason why the immobilization of pendant peptide accelerates degradation. However, there was not much difference in degradation rates when compared Ac-CRGDS incorporated hydrogels with Acryl-RGDS immobilized hydrogels.

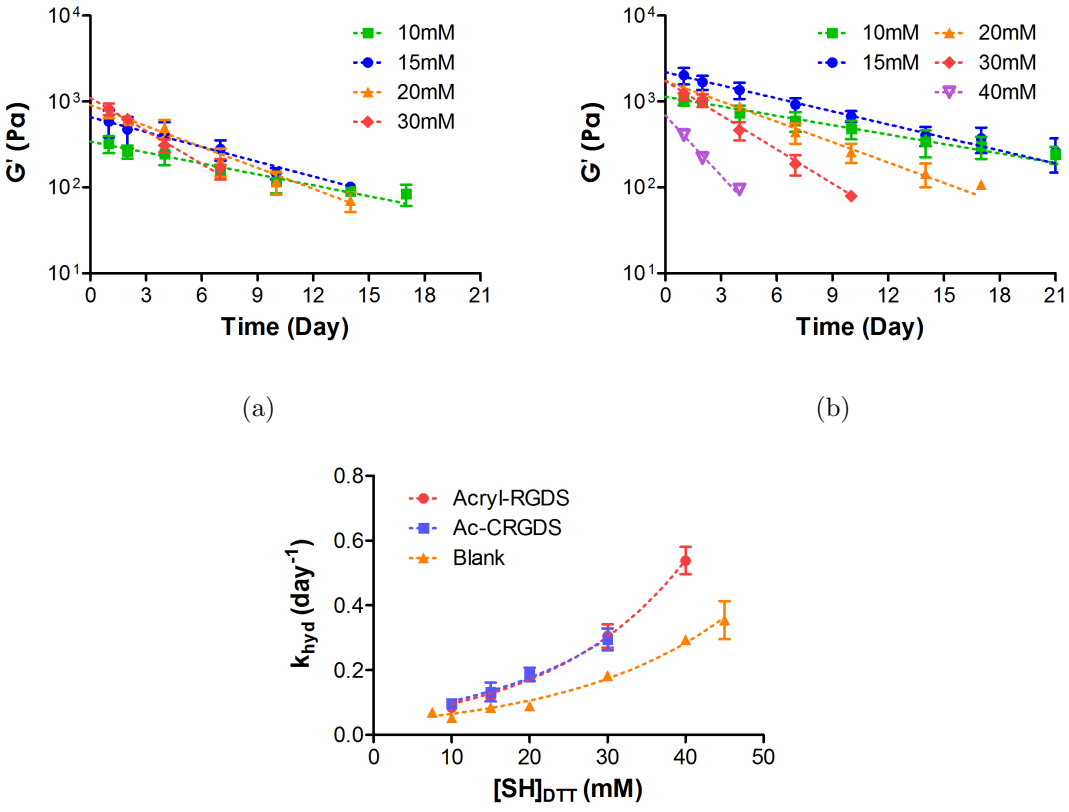

Fig. 4.8. Effect of pendant peptide (i.e., Acryl-RGDS or Ac-CRGDS) and thiol content on gel degradation. (a-b) Hydrogel elastic modulus were plotted as a function of degradation time. Hydrogels were prepared from 10 wt.% 3.4kDa PEGDA with 0.1mM eosin-Y, 0.1% NVP and 1mM pendant peptide (a) Ac-CRGDS or (b) Acryl-RGDS. Gel degradation was conducted in pH 7.4 PBS at 37°C. (d) Hydrolytic degradation rare constants (k_{hyd}) obtained from (a-b) and Figure 4.5(b) and then plotted as a function of thiol concentration.

4.2.5 Effect of NVP on Hydrogel Stiffness and Degradation

Co-monomer NVP has been reported to accelerate the gelation of acrylate-based hydrogels [31, 84]. As discussed in the last section, the incorporation of pendant peptide resulted decrease in gel stiffness. Regulating NVP concentration to compensate the negative effect of peptide on elastic modulus could be a method to obtain highly crosslinked hydrogels with incorporated pendant peptide. NVP contains one vinyl functional group in its chemical structure (Figure 1.4(e)). Unlike PEGDA macromer, NVP is a small molecular, which can spread out much more easily in the solution and therefore facilitate propagation of free radicals. The crosslinking of NVP with PEGDA also produces additional poly(NVP) kinetic chains, which have great impact on network structure, gel mechanical properties, and hydrolytic degradation rate. Here the effect of NVP on gel stiffness was evaluated via comparison of the previous PEGDA/TEA/NVP and the current PEG/DTT/NVP gelation systems (Figure 4.9). Hydrogels were fabricated from either 10 $wt.\%$ (Figure 4.9(a)) or 25 $wt.\%$ (Figure 4.9(b)) $3.4kDa$ PEGDA with 0.1 mM eosinY and 1 mM Ac-CRGDS. Previous study [31] has shown that the ratio of [NVP]/[acrylate] determines gel stiffness. In the Figure 4.9, increasing NVP concentration caused formation of stiffer hydrogels for all conditions. For example, in 10 $wt.\%$ PEGDA-DTT hydrogels, increasing NVP contents from 0.1% to 1.0% increased elastic modulus from 0.8 kPa to 25 kPa, which covered a broad range of stiffness for many applications. In addition, there was a linear relationship between gel stiffness and [NVP]/[acrylate] ratio (Table 4.3) for both chain-growth and mixed-mode polymerization. Compared with mixed-mode photopolymerization, [NVP]/[acrylate] ratio had a greater effect on gel stiffness in purely chain-growth photopolymerization, demonstrated by a larger slope in the linear regression analysis. This is possible that chain transfer events in mixed-mode polymerization reduce the effect of NVP concentration on gel stiffness.

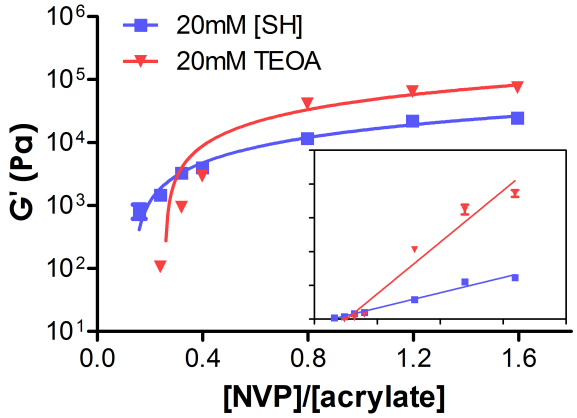

(a)

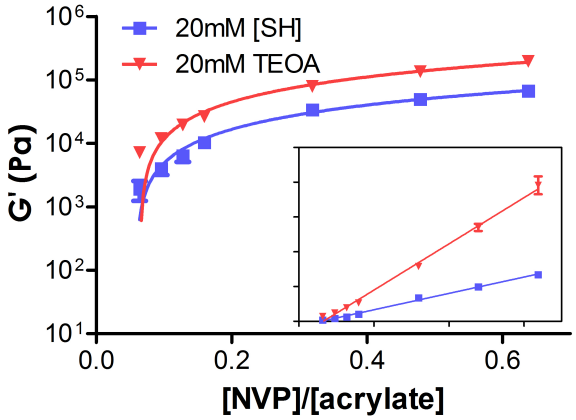

(b)

Fig. 4.9. Effect of [NVP]/[acryalte] on hydrogel equilibrium shear moduli. Hydrogels were crosslinked by chain-growth photopolymerization (20 mM TEA as co-initiator) or mixed-mode thiol-acrylate photopolymerization (20mM thiol from DTT as co-initiator) using (a) 10wt% and (b) 25wt% 3.4kDa PEGDA. The inserted figures were plotted in linear scale on both axises, showing the linear relationship between gel stiffness and ratio of [NVP]/[acryalte]. All gels were prepared with 0.1 eosinY, 1 mM Ac-CRGDS, and with 5 minutes of visible light exposure. The concentrations of NVP were 0.1, 0.15, 0.2, 0.25, 0.5, 0.75 and 1 vol.% ($N = 3, Mean \pm SD$)

Table 4.3.
Linear regression results of data presented in Figure 4.9

PEGDA ($wt.\%$)	Co-initiator	Slope	R^2
10	20 mM TEA	61190±3085	0.96
	20 mM SH_{DTT}	18090±672	0.97
25	20 mM TEA	332300±7346	0.99
	20 mM SH_{DTT}	117600±2548	0.99

Figure 4.10 shows the effect of NVP concentration on hydrolytic degradation. Conventional visible light cured PEGDA hydrogels with TEA as co-initiator was tested as control group (Figure 4.10(e)-(f)). PEGDA hydrogels were prepared from 10 $wt.\%$ (Figure 4.10(a)-(c)) or 25 $wt.\%$ (Figure 4.10(d)) PEGDA macromer with 0.1 mM eosinY and 1 mM Ac-CRGDS peptide. Bi-functional thiol DTT was added with three different concentrations, 15 mM (Figure 4.10(a)), 20 mM (Figure 4.10(b)-(d)), and 30 mM (Figure 4.10(c)). NVP was added at 0.1, 0.15, 0.2, 0.25, 0.5, 0.75, and 1 $vol.\%$. In the purely chain-growth control experiments, 20 mM of TEA was added for both groups with different concentrations of PEGDA macromer. As stated in the Section 1.1.4, all PEGDA hydrogels fabricated via mixed-mode polymerization follow the pserudo-first order degradation kinetics. As increasing of NVP concentration, the degradation rate became slower, especially when NVP concentration was higher than 0.25 $vol\%$. Thiol-acrylate hydrogels fabricated with high concentration of PEGDA macromer also exhibited slow degradation rate. In contrast, hydrogels formed via purely chain-growth using TEA were hydrolytically stable in all conditions.

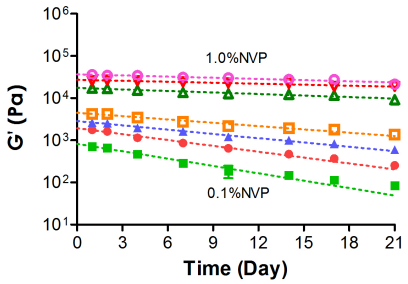

(a) 10 wt.% PEGDA, 15 mM SH_{DTT}

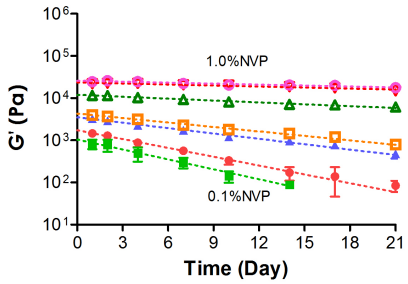

(b) 10 wt.% PEGDA, 20 mM SH_{DTT}

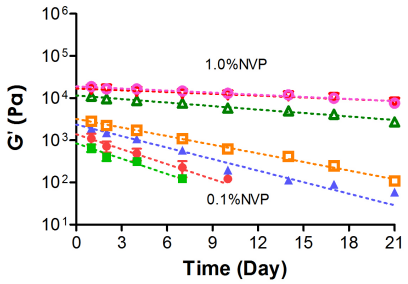

(c) 10 wt.% PEGDA, 30 mM SH_{DTT}

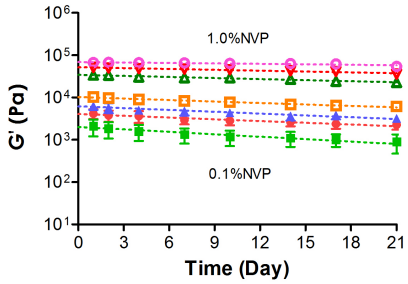

(d) 25 wt.% PEGDA, 20 mM SH_{DTT}

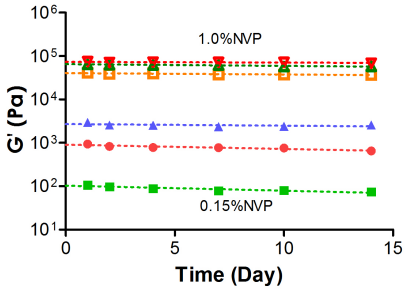

(e) 10 wt.% PEGDA, 20 mM TEA

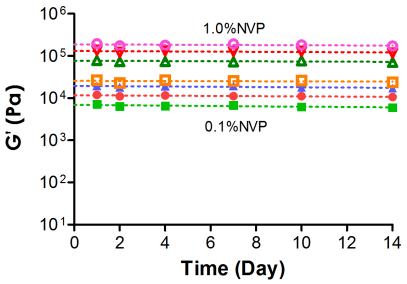

(f) 25 wt.% PEGDA, 20 mM TEA

Fig. 4.10. Effect of NVP concentration on hydrolytic degradation of mixed-mode PEGDA hydrogels immobilized with 1 mM Ac-CRGDS pendant peptide. Hydrogel elastic modulus were plotted as a function of degradation time. All hydrogels were fabricated with 0.1 mM eosinY and with 5 mins of visible light exposure. All degradation profiles were analyzed using exponential curve fitting (log scale on Y-axis). Gel degradation was conducted in pH 7.4 PBS at 37°C ($N = 3, Mean \pm SD$)

Figure 4.11 and Tabel 4.4 show the relationship between degradation rate constants (k_{hyd}) and NVP concentration. Higher concentration of thiol caused faster degradation for all NVP concentration used in this experiments. Exponential curve fitting revealed good correlations between degradation rate constants (k_{hyd}) and NVP concentration ($R^2 = 0.95 - 0.97$) for 10 $wt.\%$ thiol-acrylate hydrogels (Table 4.4). For gels formed from 25 $wt.\%$ PEGDA, the exponential fitting was less perfect because hydrogels were less degradable. As expected, chain-growth PEGDA hydrogels were not degradable as time passed (Figure 4.11(b)). According to the result in Figure 4.9, the addition of NVP significantly slowed the hydrolytically degradation rate of mixed-mode PEGDA hydrogels. This is because that NVP forms additional hydrophobic poly(NVP) kinetic chains, which restrict accessibility of water to ester bonds. In addition, increasing of NVP concentration means introducing more vinyl functional groups, which leads to formation of "chain-growth-like" network with high molecular weight kinetic chain.

Table 4.4.
Exponential curve fitting based on the data in the Figure 4.11.

PEGDA ($wt.\%$)	$[SH]_{DTT}(mM)$	Slope	R^2
10	15	-4.73±0.78	0.95
	20	-4.00±0.70	0.96
	30	-3.47±0.47	0.97
25	20	-1.75±0.32	0.92

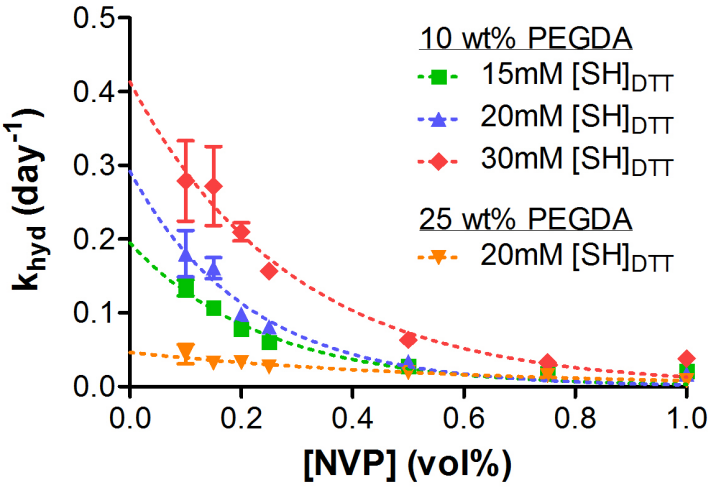

(a) Mixed-mode PEGDA hydrogels

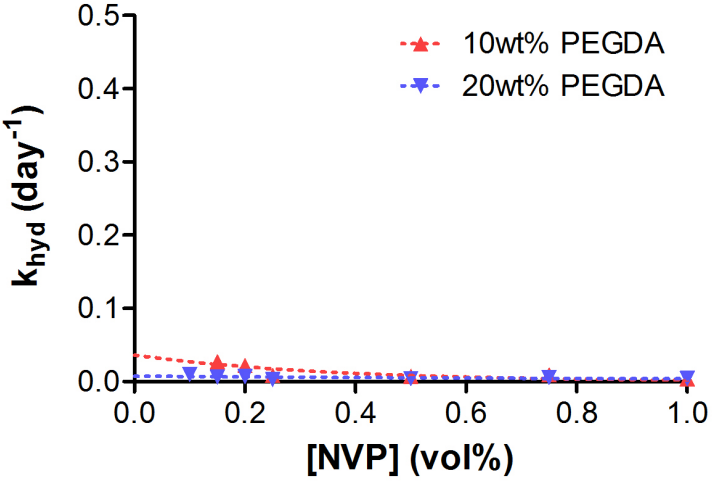

(b) Chain-growth PEGDA hydrogels

Fig. 4.11. Hydrolytic degradation rate constants (k_{hyd}) obtained from Figure 4.10 and plotted as a function of NVP concentration: (a) Mixed-mode PEGDA thiol-acrylate hydrogels, and (b) Chain-growth PEGDA hydrogels. Curves indicate an empirical fitting with an exponential relationship.

4.3 Utilize PEG-tetra-acrylate to Form Visible Light Cured Thiol-acrylate Hydrogels

As discussed above, PEGDA hydrogels can be fabricated via mixed-mode polymerization under visible light exposure and properties of such PEGDA hydrogels can be tuned by many methods. However, forming PEGDA hydrogel via mixed-mode photopolymerization requires usage of high concentration of PEGDA macromer (at least 10 $wt.\%$). Therefore, in this section, formation of thiol-acrylate hydrogels using PEG-tetra-acrylate (PEG4A) macromers was investigated. Since PEG4A has two more acrylate functional groups than PEGDA, it should form highly crosslinked network with relatively low concentration of macromer.

4.3.1 Effect of Vinyl Moiety on Hydrogel Gelation

As mentioned in earlier Section 1.1.1, many multi-functional PEG-derivatives have been investigated for hydrogen fabrication, including PEG-tetra-allylther (PEG-4AE), PEG-tetra-methacrylate (PEG4MA), PEG-tetra-acryalmide (PEG4AA), and PEG-tetra-acrylate (PEG4A). Figure 4.12 shows the in situ rheometry data of thiol-vinyl hydrogels using these four PEG macromers. All hydrogels were prepared from 4 $wt.\%$ PEG macromer, 4 mM DTT with 0.1 mM eosinY and 1.0% NVP. The use of PEG4A yielded the fastest gelation kinetics (F3 in Table 4.5), followed by PEG4AA (F8 in Table 4.5) and PEG4MA (F9 in Table 4.5). PEG4AE cannot form hydrogels within 10 minutes via mixed-mode mechanism in this case (F10 in Table 4.5). Although all of these four PEG macromers contain vinyl functional groups in their chemical structures (Figure 1.2), the reactivity of the vinyl moieties affected hydrogel crosslinking efficiency, which resulted in different gel points during gelation. Since PEG4A had fastest gelation rate, it was chosen as the macromer used for the rest of study.

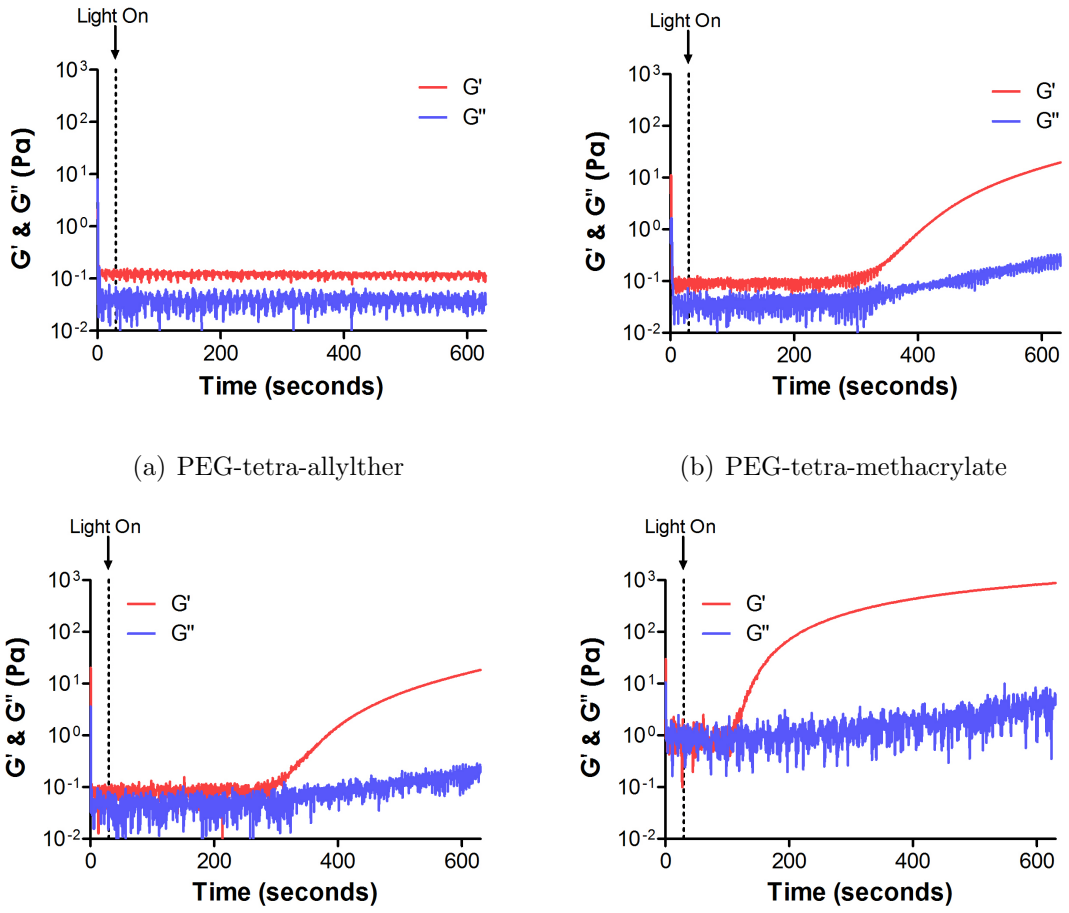

(a) PEG-tetra-allylther

(b) PEG-tetra-methacrylate

(c) PEG-tetra-acrylamide

(d) PEG-tetra-acrylate

Fig. 4.12. In situ photorheometry data showing the effect of PEG macromer vinyl moiety on the evolution of elastic/viscous (G'/G'') modulus. Hydrogels were prepared from 4 wt.% (a) PEG-tetra-allylther, (b) PEG-tetra-methacrylate, (c) PEG-tetra-acrylamide and (d) PEG-tetra-acrylate using 4 mM DTT (8 mM thiol), 0.1 mM eosinY and 1.0% NVP.

Table 4.5.
Gel points for gel formulations used in in situ photorheometry

Formulation	Macromer	f_A^a	Co-initiator/ Cross-linker[b]	f_B^b	NVP ($vol\%$)	Gel point (sec)
F1	PEG4A	4	DTT	2	0	430±38
F2	PEG4A	4	DTT	2	0.1	231±12
F3	PEG4A	4	DTT	2	1.0	92±11
F4	PEG4A	4	Cysteine	1	1	250±14
F5	PEG4A	4	CGGGC	2	1	26±5
F6	PEG4A	4	KCGPQGIWGQCK	2	0.1	86±3
F7	PEG4A	4	KCGPQGIWGQCK	2	1	19±2
F8	PEG4AA	4	DTT	2	1	275±21
F9	PEG4MA	4	DTT	2	1	305±36
F10	PEG4AE	4	DTT	2	1	> 600
F11[c]	PEG4A	4	-	-	0.1	78±4
F12[c]	PEG4A	4	-	-	1	13±1

[a] f_A and f_B are the functionality of the macromers and crosslinkers, respectively.

[b] Thiol concentration = 8 mM.

[c] Chain-growth photopolymerization using 8 mM TEA as co-initiator.

4.3.2 Effect of NVP on Hydrogel Properties

Theoretically, thiyl radicals generated by hydrogen abstraction reaction should be able to initiate polymerization, like what happened in step-growth thiol-acrylate gelation using PEG-tetra-norbornene [34]. However, acrylates on PEG4A exhibited slow reaction kinetics under visible light exposure (Figure 4.13(a)), which suggested a need for accelerating gelation rate. Since NVP is a common co-monomer that

used to facilitate gelation kinetics in conventional chain-growth polymerization [31], it might function to accelerate gelation rate as well in mixed-mode polymerization. Here hydrogels were prepared from 4 $wt.\%$ PEG4A, 4 mM DTT and 0.1 mM eosinY with different concentrations of NVP. Indeed, adding 0.1% or 1.0% NVP decreased gel points from ~430 sec to ~231 and ~92 sec respectively (Figure 4.13). The reason why NVP increased gelation rate could be rapid diffusion of radicals [28,31] as mentioned in previous Section 4.2.5.

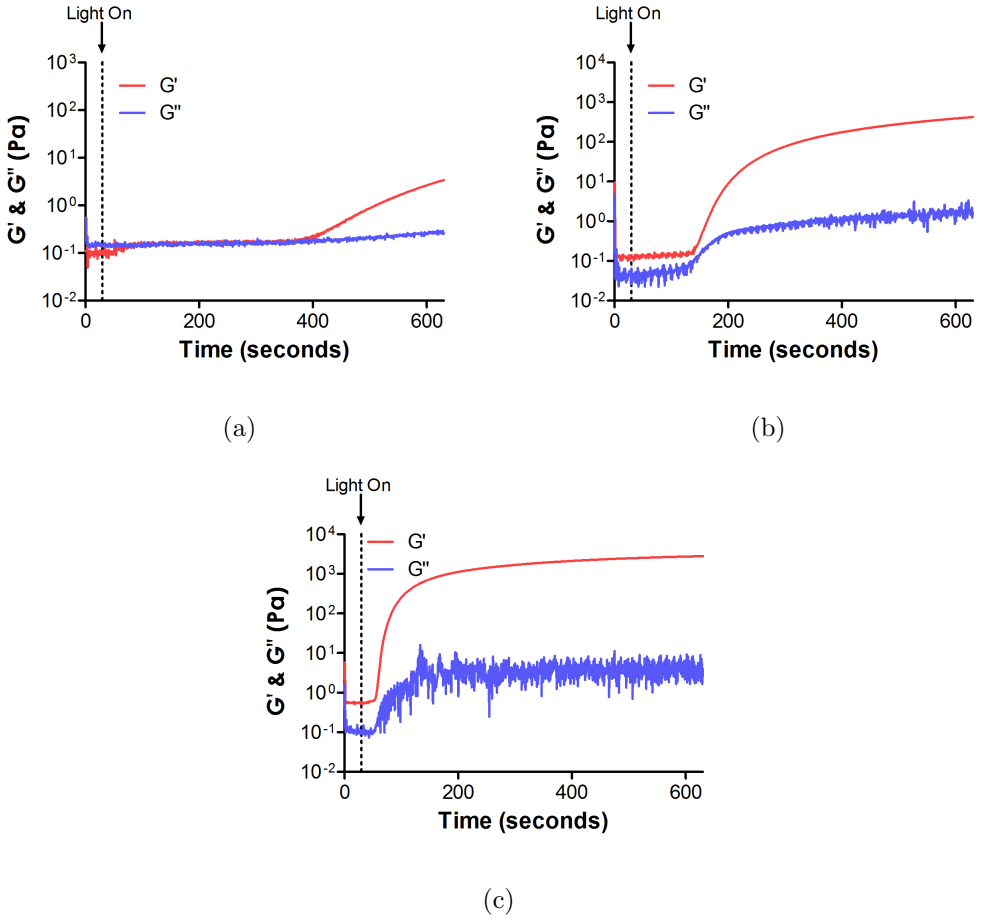

Fig. 4.13. In situ photorheometry data showing the effect of NVP concentration on the evolution of elastic/viscous (G'/G'') modulus of mixed-mode PEG4A hydrogels. Hydrogels were fabricated from 4wt.% PEG4A with 4 mM DTT, 0.1 mM eosinY and with (a) 0% or (b) 0.1% and (c) 1.0% NVP.

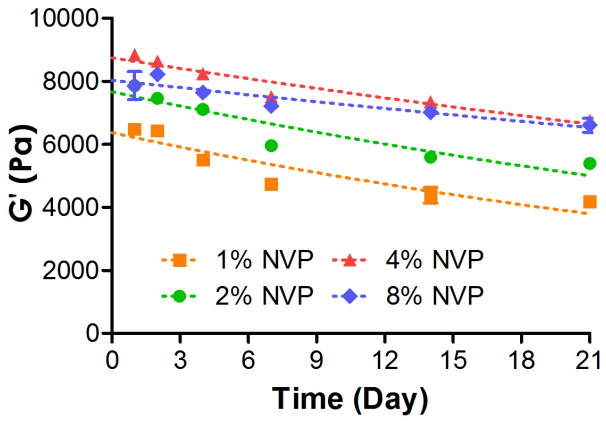

(a)

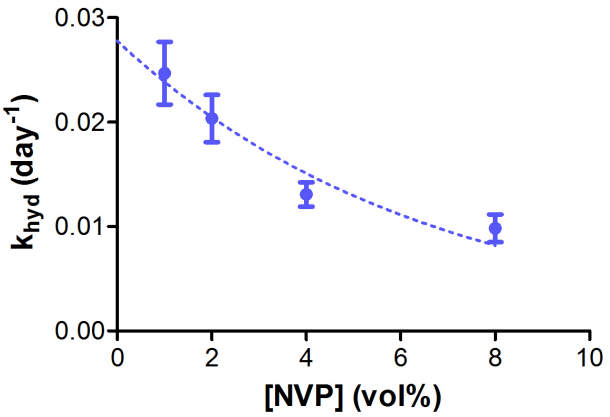

(b)

Fig. 4.14. Effect of NVP concentration on gel degradation of mixed-mode PEG-tetra-acrylate hydrogels. (a) Hydrogels elastic modulus were plotted as a function of degradation time. All gels were prepared from 4wt.% PEG4A with 4 mM CGGGC, 0.1 mM eosinY and 5 min of visible light exposure. NVP was added at 1%, 2%, 4% and 8%. All degradation profiles were conducted using exponential curve fitting (log scale on Y-axis). Gel degradation was conducted in pH 7.4 PBS at 37°C. (b) Hydrolytic degradation rate constants (k_{hyd}) were obtained from (a) and plotted as a function of NVP concentration with an exponential growth fitting ($N = 3, Mean \pm SD$).

At fixed concentration of PEG4A and thiol-containing crosslinker, increasing NVP content in the precursor solution increased vinyl-to-thiol ratio (Table 4.6), which dragged the network crosslinking to become a more "chain-growth like" structure with additional poly(NVP) kinetic chains. These kinetic chains made hydrogels with higher elastic modulus and slower degradation rate (Figure 4.14). The results also show the exponential relationship between degradation rate constants and NVP contents, which is consistent with previous result when using PEGDA as macromer (Section 4.2.5).

Table 4.6.
Functional group concentrations and vinyl-to-thiol ratios

Tetra-vinyl		NVP		Di-thiol	Ratio $\frac{[vinyl]}{[thiol]}$
$wt\%$	[acrylate] (mM)	$vol.\%$	[vinyl] (mM)	[thiol] (mM)	
4	8	0	0	8	1
		0.1	9.38	4	4.35
		0.1	9.38	6	2.90
		0.1	9.38	8	2.17
		1	93.8	4	25.45
		1	93.8	6	16.97
		1	93.8	8	12.73

4.3.3 Effect of Thiol Functionality and Chemistry on Hydrogel Properties

The thiol containing molecules used as co-initiator and crosslinkers can also affect gelation efficiency. As showed in the Figure 4.15, when using different crosslinkers (e.g. Cysteine, DTT, CGGGC and CGCGC), the gelation rates were different. With mono-thiol cysteine, gelation did not occur until after 250 *sec* of light exposure (F4

in Table 4.5). When mono-thiol cysteine reacted with acrylate via step-growth polymerization, it formed an effective termination in the network. In this case, cysteine only functioned as co-initiator to generate free radicals, but not as crosslinker. The later increase of elastic modulus is like due to homopolymerization reaction between acrylates. On the other hands, bis-cysteine containing peptide (e.g. CGGGC) could act as both co-initiator and crosslinkers. With peptide CGGGC, gelation occurred at about 26 *sec* in the present of 1.0% NVP (F5 in Table 4.5). Furthermore, using CGCGC yielded even faster gelation. This is because that CGCGC has three thiol functional groups in its structure, which means it has more reactive spots to crosslink with acrylates forming tighter network.

In addition, the results also indicated that the crosslinking efficiency between acrylate and thiol was affected by the chemistry property of thiol containing molecules. For example, hydrogel properties, including stiffness and degradation rate, were still different, although all of the crosslinkers contained two thiol functional groups (Figure 4.16). The use of MMP-sensitive peptide KCGPQGIWCGCK (F7 in Tabel 4.5) or CGGGC yielded gel points of 19 or 26 *sec* respectively, while the gel point was 92 *sec* when using DTT as crosslinkers. This is probably because that more intermolecular disulfide bonds forming in DTT than in bis-cysteine containing peptides during this radical-mediated reaction, reducing the available thiyl radicals for crosslinking. The same results were found in previous research done by Salinas and Anseth using UV-mediated thiol-acrylate hydrogels [46] and also in work done by Lutolf and Hubbel using Michael type addition hydrogels [85]. In addition, some amino acid side groups in peptides might also affect the gelation process via changing the reactivity of cysteine deprotonation. For example, using CGGYC as crosslinker instead of CGGGC, with only one amino acid difference, could significantly increase crosslinking density, resulting in higher elastic modulus (Figure 4.16(a)) and shower degradation rate (Figure 4.16(d)).

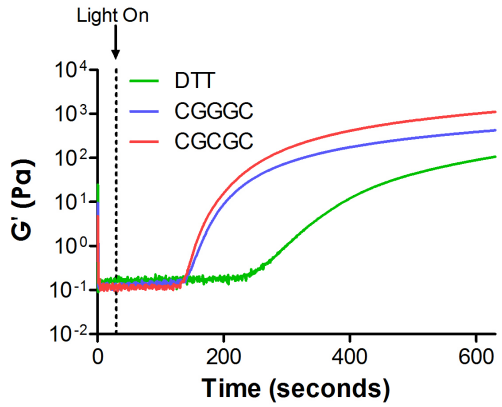

(a)

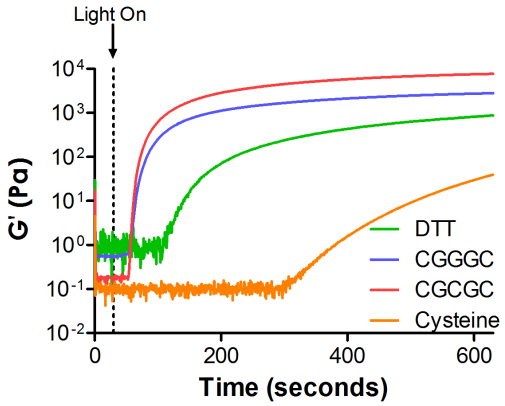

(b)

Fig. 4.15. In situ photorheometry data showing the effect of thiol functionality on hydrogel gelation. Crosslinkers with different number of thiol functional group were Cysteine, DTT, CGGGC and CGCGC. Hydrogels were prepared from 4 wt.% PEG-tetra-acrylate with 4 mM crosslinkers, 0.1 mM eosinY and (a) 0.1 vol% or (b) 1.0 vol% NVP.

In order to compare, gel points of conventional chain-growth polymerization using 4 $wt.\%$ PEG4A, 8 mM TEA and 0.1% or 1.0% NVP (F11 and F12 in Table 4.5 respectively) was also investigated. Gelation rates of purely chain-growth polymerization with TEA (gel point $\approx$ 78 or 13 with 0.1% or 1.0% NVP respectively) were quite similar to those of mixed-mode polymerizations using bis-cysteine peptides (using KCGPQGIWGQCK, gel point $\approx$ 86 or 19 with 0.1% or 1.0% NVP).

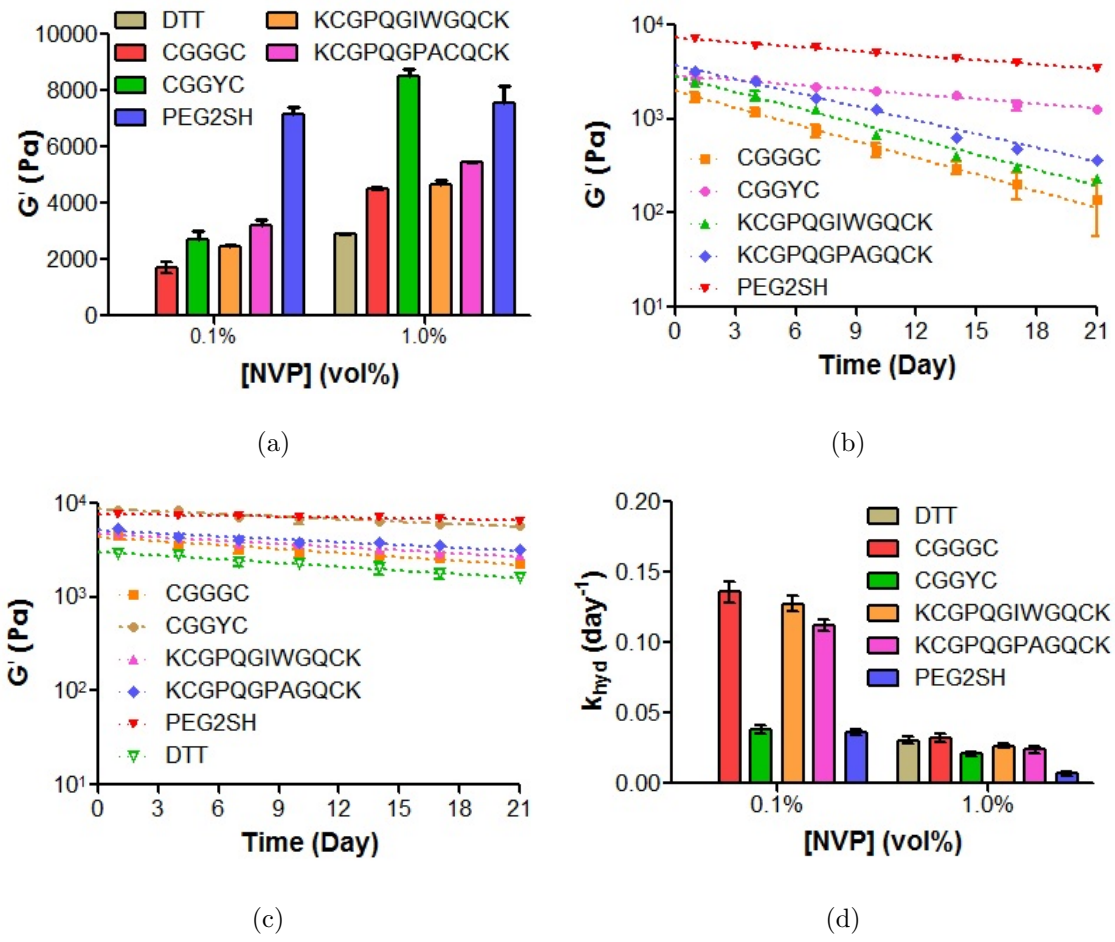

Fig. 4.16. Effect of thiol chemistry on (a) elastic modulus (G') and (b-d) hydrolytic degradation of mixed-mode PEG-tetra-acrylate hydrogels. All crosslinkers, including DTT, CGGGC, CGGYC, KCGPQGIWGQCK, KCGPQGPAGQCK and PEG-dithiol, have two thiol functional groups. Hydrogels were fabricated from 4wt.% PEG4A with 4 mM crosslinkers, 0.1 mM eosinY with (b) 0.1% or (c) 1.0% NVP. %. All degradation profiles were conducted using exponential curve fitting (log scale on Y-axis). Gel degradation was conducted in pH 7.4 PBS at 37°C. (d) Hydrolytic degradation rate constants (k_{hyd}) obtained from (b) and (c).

4.3.4 Effect of Thiol Concentration on Hydrogel Properties

Next, the effect of thiol concentration on the property of visible light cured thiol-acrylate hydrogels was examined. With the same PEG4A concentration (i.e., 4 $wt.\%$, total 8 mM acrylate), increasing thiol concentration from 4 mM to 8 mM (that is 2 to 4 mM CGGGC) decreased gel stiffness and equilibrium gel swelling ratios (Figure 4.17), suggesting decrease in network crosslinking density. Even in the presence of 1.0% NVP, where the concentration of vinyl functional groups was about 12 to 25-fold higher than thiol concentration, the change of thiol content still affected the stiffness and swelling of hydrogels (Figure 4.17). This was because that higher concentration of thiol in precursor solution resulted more acrylates participating in step-growth polymerization, forming network with higher amounts of thiol-ester linkages. As a decreased thiol content, polymerization kinetics shifted toward chain-growth polymerization, which produced dense and hydrophobic kinetic chains. These kinetic chains led to stiffer and less swollen hydrogel.

Figure 4.18 and Table 4.7 shows the effect of thiol concentration on hydrogel degradation. Theoretically, hydrogels formed by PEG4A and thiol-containing crosslinker would degrade following bulk degradation mechanism as mentioned in Section 1.1.4. Hydrogel elastic modulus (G') were plotted as function of degradation time (Figure 4.18(a)-(b)). And as thiol content increased, hydrogels degraded with faster rate at both NVP concentrations. This phenomenon was due to the formation of more thiol-ether-ester bonds with higher amounts of peptide CGGGC. Since the hydrolytic degradation rate of hydrogels following bulk degradation was determined by the concentration of hydrolytically labile units, higher thiol-ester bond concentration would result in faster degradation rate.

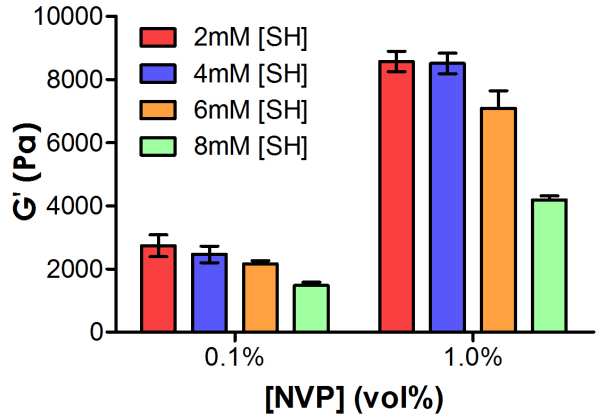

(a)

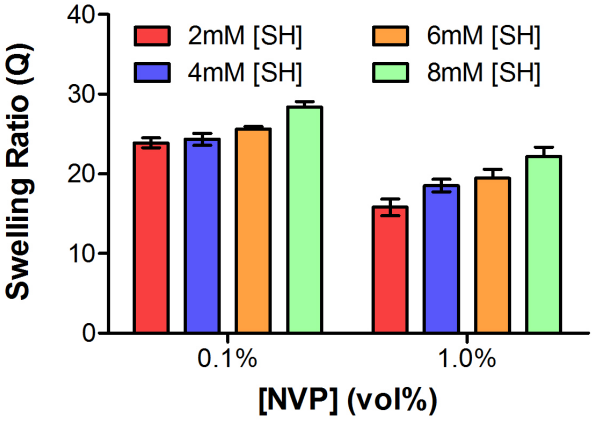

(b)

Fig. 4.17. Effect of thiol concentration on gel properties : (a) Equilibrium shear modulus (G') and (b) Swelling ratio (Q). Hydrogels were prepared from 4wt.% PEG4A with 0.1 mM eosinY and 5 min of visible light exposure. CGGGC was added at 1, 2, 3 and 4 mM, that is 2, 4, 6 and 8 mM total thiol. All properties were measured at day-1 post gelation.

The degradation behavior of PEG4A hydrogels can be perfectly described by equation 4.1 ($R^2 = 0.95 \sim 0.99$, Table 4.7):

$$\frac{G'}{G'_0} = e^{-kt}$$

However, the degradation profiles of hydrogels prepared with 1.0% NVP fit less perfectly using exponential curve fitting ($R^2 = 0.88 \sim 0.94$). It was likely that she hydrolytic degradation of PEG4A hydrogel with higher NVP concentration was affected by the formation of dense and hydrophobic poly(NVP) kinetic chains. In addition, the degradation rate constants (k_{hyd}) (Figure 4.18(c)) of hydrogels crosslinked with 0.1% NVP were 1.68 to 3.42 fold higher than that in hydrogels with 1.0% NVP (Table 4.7). One possible explanation is that poly(NVP) kinetic chains slows down the degradation rate.

Table 4.7.
Hydrolyltic degradation rate constants of visible light-mediated thiol-acrylate hydrogels with different thiol and NVP concentrations (with CGGGC as crosslinker).

NVP (%)	[acrylate] (mM)	[SH] (mM)	k_{hyd} (day^{-1})	R^2
0.1	8	4	0.032±0.002	0.95
		6	0.060±0.003	0.97
		8	0.168±0.005	0.99
1.0	8	4	0.019±0.001	0.89
		6	0.026±0.002	0.91
		8	0.049±0.003	0.94

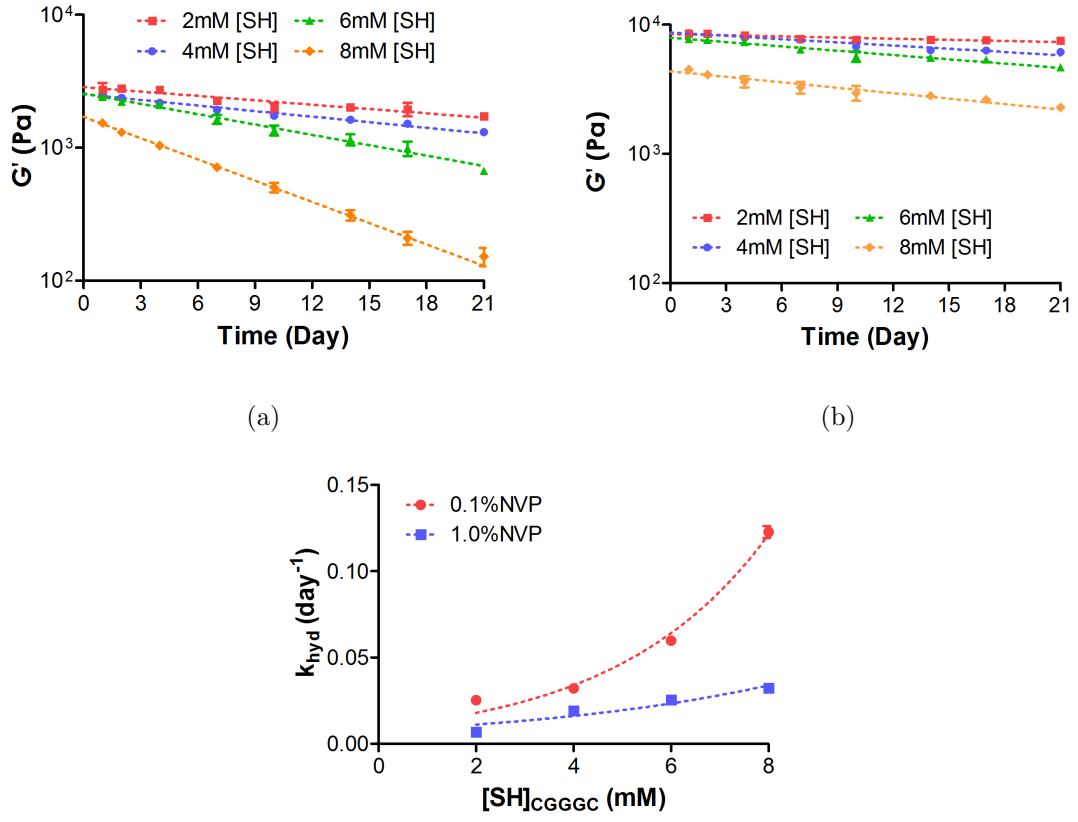

Fig. 4.18. Effect of thiol concentration on gel degradation. (a-b) Hydrogel elastic modulus (G') were plotted as a function of degradation time. All gels were prepared from 4 wt.% PEG4A with 0.1 mM eosinY and (a) 0.1% or (b) 1.0% NVP. CGGGC was added at 1, 2, 3 and 4 mM, that is 2, 4, 6 and 8 mM total thiol respectively. (c) Hydrolytic degradation rate constants (k_{hyd}) were obtained from (a-b) and plotted as a function of thiol concentration with an exponential growth fitting ($N = 3, Mean \pm SD$).

4.3.5 Effect of Macromer Composition on Hydrogel Hydrolytic Stability

Hydrogels presented before are all degradable. However, non-degradable hydrogels are needed in some biomedical applications, such as islets encapsulation to prevent immune response. Therefore, a non-degradable hydrogel was also developed in this thesis using PEG-tetra-acrylamide (PEG4AA) with non-cleavable peptides (Figure

4.19(a)). Since there is no thiol-ether-ester bond in the network, hydrogels are hydrolytically stable. For example, the elastic modulus (G') of hydrogels prepared from 4 $wt.\%$ PEG4AA and 4 mM CGGGC remained relatively stable as degradation time regardless of NVP concentration incorporated (Figure 4.19(b)). In addition, increasing NVP concentration increased gel stiffness as expected. However, this effect reached maximum at 4% NVP. Further changing NVP concentration from 4% to 8% did not increase elastic modulus. As mentioned before, NVP has one vinyl functional group that could react with two vinyl groups. Therefore, the functionality of NVP is two, which means that it could create linear poly(NVP) kinetic chains at higher concentrations. Such linear structures did not contribute to the stiffness of hydrogels. This was likely why further increasing NVP concentration did not cause additional increase in gel elastic modulus. In addition, under the same conditions, hydrogels prepared from PEG4AA possess weaker mechanical property than PEG4A hydrogels due to the lower reactivity of acrylamide as discussed earlier (Table 4.5 and Figure 4.12).

(a)

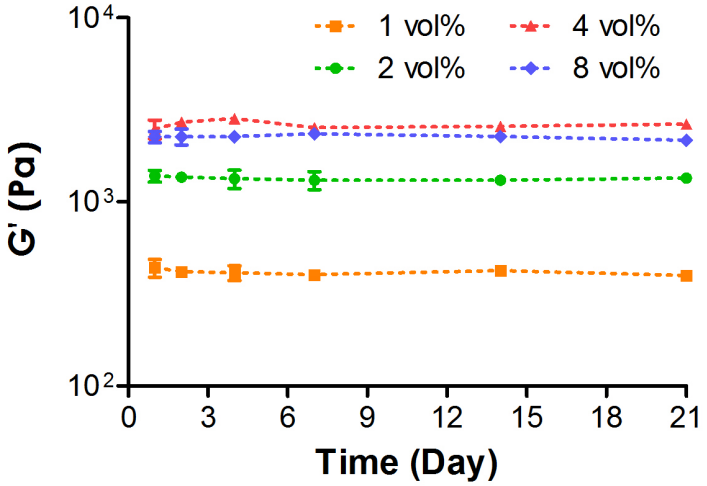

(b)

Fig. 4.19. (a) Structure of non-degradable thiol-ether-acrylamide. (b) Relatively stable shear moduli as a function of time and NVP concentration for hydrogels prepared from 4 wt.% PEG4AA (8 mM acrylate) and 4 mM CGGGC (8 mM thiol) with 0.1 mM eosinY. NVP was added at 1%, 2%, 4% and 8%. Hydrogel elastic modulus (G') were plotted as a function of degradation time.

5. CONCLUSIONS

The aim of this study was to develop visible light-mediated thiol-vinyl hydrogels via mixed-mode photopolymerization. Compared to conventional purely chain-growth polymerization, high concentration of toxic TEA was replaced by thiol-containing molecules, which improve the biocompatibility of fabrication process. Here, PEG-diacrylate (PEGDA) hydrogels could be fabricated using eosinY as initiator, NVP as co-monomer, thiol-containing molecules (e.g. DTT or cysteine containing peptides) as crosslinker and co-initiator, when thiol-to-vinyl were in a certain range. The gelation kinetics and gel properties could be controlled by changing eosinY concentration, molecular weight of macromer, NVP content, crosslinker concentration and polymerization time. Since many previous researches incorporated bioactive motifs into hydrogels, the effect of incorporated pendant peptide RGD on hydrogel properties was also investigated in this thesis. Immobilization of pendant peptide decreased gel stiffness and accelerated hydrogel degradation.

Forming highly crosslinked hydrogels required high concentration of macromer PEGDA, at least 10 $wt.\%$. Therefore, in order to fabricate hydrogels with lower macromer content, 4-arm vinyl-based PEG macromers were used. Among the four macromers, PEG-tetra-acrylate (PEG4A) exhibited fastest gelation. The functionality and reactivity of thiol-containing molecule also affected gelation rate and hydrogel properties. Like PEGDA hydrogels, the properties of PEG4A hydrogels could be tuned by altering concentration of NVP and thiol crosslinker.

In addition, non-degradable hydrogels prepared from PEG-tetra-acrylamide were also presented in this thesis. Due to the formation of thiol-ether-acrylamide bond instead of thiol-ether-ester bond, PEG4AA hydrogels are hydrolytically stable compared to PEG-acrylate hydrogels. Hydrogels fabricated via this visible light-mediated

mixed-mode photopolymerization have potentials in many biomedical applications, such as cell encapsulation and drug delivery.

LIST OF REFERENCES

LIST OF REFERENCES

[1] O. Wichterle and D. Lim, "Hydrophilic gels for biological use," *Nature*, vol. 185, p. 117, Jan 1960.

[2] S. C. Lee, I. K. Kwon, and K. Park, "Hydrogels for delivery of bioactive agents: a historical perspective," *Adv Drug Deliv Rev*, vol. 65, no. 1, pp. 17–20, Jan 2013.

[3] S. Van Vlierberghe, P. Dubruel, and E. Schacht, "Biopolymer-based hydrogels as scaffolds for tissue engineering applications: A review," *Biomacromolecules*, vol. 12, no. 5, pp. 1387–1408, 2011.

[4] K. Y. Lee and D. J. Mooney, "Hydrogels for tissue engineering," *Chemical reviews*, vol. 101, no. 7, pp. 1869–1880, 2001.

[5] D.-C. Chen, Y.-L. Lai, S.-Y. Lee, S.-L. Hung, and H.-L. Chen, "Osteoblastic response to collagen scaffolds varied in freezing temperature and glutaraldehyde crosslinking," *Journal of Biomedical Materials Research Part A*, vol. 80A, no. 2, pp. 399–409, 2007.

[6] B. Chevallay, N. Abdul-Malak, and D. Herbage, "Mouse fibroblasts in long-term culture within collagen three-dimensional scaffolds: Influence of crosslinking with diphenylphosphorylazide on matrix reorganization, growth, and biosynthetic and proteolytic activities," *Journal of Biomedical Materials Research*, vol. 49, no. 4, pp. 448–459, 2000.

[7] S. Gorgieva and V. Kokol, "Collagen vs. gelatine-based biomaterials and their biocompatibility: Review and perspectives," *Biomaterials Applications for Nanomedicine, InTech*, 2011.

[8] J. A. Burdick and G. D. Prestwich, "Hyaluronic acid hydrogels for biomedical applications," *Advanced Materials*, vol. 23, no. 12, pp. H41–H56, 2011.

[9] T. A. Ahmed, E. V. Dare, and M. Hincke, "Fibrin: a versatile scaffold for tissue engineering applications," *Tissue Engineering Part B: Reviews*, vol. 14, no. 2, pp. 199–215, 2008.

[10] A. D. Augst, H. J. Kong, and D. J. Mooney, "Alginate hydrogels as biomaterials," *Macromolecular Bioscience*, vol. 6, no. 8, pp. 623–633, 2006.

[11] A. Balgude, X. Yu, A. Szymanski, and R. Bellamkonda, "Agarose gel stiffness determines rate of drg neurite extension in 3d cultures," *Biomaterials*, vol. 22, no. 10, pp. 1077 – 1084, 2001, neural Tissue Engineering.

[12] A. Chenite, C. Chaput, D. Wang, C. Combes, M. Buschmann, C. Hoemann, J. Leroux, B. Atkinson, F. Binette, and A. Selmani, "Novel injectable neutral solutions of chitosan form biodegradable gels in situ," *Biomaterials*, vol. 21, no. 21, pp. 2155–2161, 2000.

[13] K. Ono, Y. Saito, H. Yura, K. Ishikawa, A. Kurita, T. Akaike, and M. Ishihara, "Photocrosslinkable chitosan as a biological adhesive," *Journal of Biomedical Materials Research*, vol. 49, no. 2, pp. 289–295, 2000.

[14] K. Y. Lee and D. J. Mooney, "Hydrogels for tissue engineering," *Chemical Reviews*, vol. 101, no. 7, pp. 1869–1880, 2001.

[15] Y. P. Jung, J.-H. Kim, D. S. Lee, and Y. H. Kim, "Preparation and properties of modified phema hydrogel with sulfonated peg graft," *Journal of Applied Polymer Science*, vol. 104, no. 4, pp. 2484–2489, 2007.

[16] K. H. Hong, Y.-S. Jeon, D. J. Chung, and J.-H. Kim, "Drug release characteristics of modified phema hydrogel containing thermo-responsive pluronic copolymer," *Macromolecular Research*, vol. 18, no. 2, pp. 204–207, 2010.

[17] J. Xu, X. Li, and F. Sun, "Cyclodextrin-containing hydrogels for contact lenses as a platform for drug incorporation and release," *Acta biomaterialia*, vol. 6, no. 2, pp. 486–493, 2010.

[18] S. M. LaNasa, I. T. Hoffecker, and S. J. Bryant, "Presence of pores and hydrogel composition influence tensile properties of scaffolds fabricated from well-defined sphere templates," *Journal of Biomedical Materials Research Part B: Applied Biomaterials*, vol. 96B, no. 2, pp. 294–302, 2011.

[19] T. Hatakeyema, J. Uno, C. Yamada, A. Kishi, and H. Hatakeyama, "Gel–sol transition of poly(vinyl alcohol) hydrogels formed by freezing and thawing," *Thermochimica acta*, vol. 431, no. 1, pp. 144–148, 2005.

[20] P. Martens and K. Anseth, "Characterization of hydrogels formed from acrylate modified poly(vinyl alcohol) macromers," *Polymer*, vol. 41, no. 21, pp. 7715–7722, 2000.

[21] I. Gibas and H. Janik, "Review: Synthetic polymer hydrogels for biomedical applications," 2010.

[22] H. Vihola, A. Laukkanen, L. Valtola, H. Tenhu, and J. Hirvonen, "Cytotoxicity of thermosensitive polymers poly(n-isopropylacrylamide), poly(n-vinylcaprolactam) and amphiphilically modified poly(n-vinylcaprolactam)," *Biomaterials*, vol. 26, no. 16, pp. 3055 – 3064, 2005.

[23] C.-C. Lin and K. S. Anseth, "Peg hydrogels for the controlled release of biomolecules in regenerative medicine," *Pharmaceutical research*, vol. 26, no. 3, pp. 631–643, 2009.

[24] J. Li and W. J. Kao, "Synthesis of polyethylene glycol derivatives and pegylated-peptide biopolymer conjugates," *Biomacromolecules*, vol. 4, no. 4, pp. 1055–1067, 2003.

[25] J. Lei, C. Mayer, V. Freger, and M. Ulbricht, "Synthesis and characterization of poly(ethylene glycol) methacrylate based hydrogel networks for anti-biofouling applications," *Macromolecular Materials and Engineering*, vol. 298, no. 9, pp. 967–980, 2013.

[26] S. Lin-Gibson, R. L. Jones, N. R. Washburn, and F. Horkay, "Structure-property relationships of photopolymerizable poly (ethylene glycol) dimethacrylate hydrogels," *Macromolecules*, vol. 38, no. 7, pp. 2897–2902, 2005.

[27] M. Browning, T. Wilems, M. Hahn, and E. Cosgriff-Hernandez, "Compositional control of poly (ethylene glycol) hydrogel modulus independent of mesh size," *Journal of Biomedical Materials Research Part A*, vol. 98, no. 2, pp. 268–273, 2011.

[28] M. V. Turturro, S. Sokic, J. C. Larson, and G. Papavasiliou, "Effective tuning of ligand incorporation and mechanical properties in visible light photopolymerized poly (ethylene glycol) diacrylate hydrogels dictates cell adhesion and proliferation," *Biomedical Materials*, vol. 8, no. 2, p. 025001, 2013.

[29] B. Yañez-Soto, S. J. Liliensiek, C. J. Murphy, and P. F. Nealey, "Biochemically and topographically engineered poly(ethylene glycol) diacrylate hydrogels with biomimetic characteristics as substrates for human corneal epithelial cells," *Journal of Biomedical Materials Research Part A*, vol. 101A, no. 4, pp. 1184–1194, 2013.

[30] A. E. Rydholm, S. K. Reddy, K. S. Anseth, and C. N. Bowman, "Development and characterization of degradable thiol-allyl ether photopolymers," *Polymer*, vol. 48, no. 15, pp. 4589 – 4600, 2007.

[31] D. L. Elbert and J. A. Hubbell, "Conjugate addition reactions combined with free-radical crosslinking for the design of materials for tissue engineering," *Biomacromolecules*, vol. 2, no. 2, pp. 430–441, 2001.

[32] M. B. Browning and E. Cosgriff-Hernandez, "Development of a biostable replacement for pegda hydrogels," *Biomacromolecules*, vol. 13, no. 3, pp. 779–786, 2012.

[33] E. A. Phelps, N. O. Enemchukwu, V. F. Fiore, J. C. Sy, N. Murthy, T. A. Sulchek, T. H. Barker, and A. J. García, "Maleimide cross-linked bioactive peg hydrogel exhibits improved reaction kinetics and cross-linking for cell encapsulation and in situ delivery," *Advanced Materials*, vol. 24, no. 1, pp. 64–70, 2012.

[34] C.-C. Lin, A. Raza, and H. Shih, "Peg hydrogels formed by thiol-ene photo-click chemistry and their effect on the formation and recovery of insulin-secreting cell spheroids," *Biomaterials*, vol. 32, no. 36, pp. 9685 – 9695, 2011.

[35] M. Lutolf, J. Lauer-Fields, H. Schmoekel, A. Metters, F. Weber, G. Fields, and J. Hubbell, "Synthetic matrix metalloproteinase-sensitive hydrogels for the conduction of tissue regeneration: engineering cell-invasion characteristics," *Proceedings of the National Academy of Sciences*, vol. 100, no. 9, pp. 5413–5418, 2003.

[36] M. Lutolf and J. Hubbell, "Synthetic biomaterials as instructive extracellular microenvironments for morphogenesis in tissue engineering," *Nature biotechnology*, vol. 23, no. 1, pp. 47–55, 2005.

[37] J. H. Ward and N. A. Peppas, "Preparation of controlled release systems by free-radical uv polymerizations in the presence of a drug," *Journal of Controlled Release*, vol. 71, no. 2, pp. 183–192, 2001.

[38] D. L. Hern and J. A. Hubbell, "Incorporation of adhesion peptides into nonadhesive hydrogels useful for tissue resurfacing," *Journal of Biomedical Materials Research*, vol. 39, no. 2, pp. 266–276, 1998.

[39] A. S. Sawhney, C. P. Pathak, and J. A. Hubbell, "Bioerodible hydrogels based on photopolymerized poly(ethylene glycol)-co-poly(alpha-hydroxy acid) diacrylate macromers," *Macromolecules*, vol. 26, no. 4, pp. 581–587, 1993.

[40] A. Metters and J. Hubbell, "Network formation and degradation behavior of hydrogels formed by michael-type addition reactions," *Biomacromolecules*, vol. 6, no. 1, pp. 290–301, 2005.

[41] Y. Fu and W. J. Kao, "In situ forming poly(ethylene glycol)-based hydrogels via thiol-maleimide michael-type addition," *Journal of Biomedical Materials Research Part A*, vol. 98A, no. 2, pp. 201–211, 2011.

[42] A. B. Pratt, F. E. Weber, H. G. Schmoekel, R. Müller, and J. A. Hubbell, "Synthetic extracellular matrices for in situ tissue engineering," *Biotechnology and Bioengineering*, vol. 86, no. 1, pp. 27–36, 2004.

[43] B. D. Fairbanks, M. P. Schwartz, A. E. Halevi, C. R. Nuttelman, C. N. Bowman, and K. S. Anseth, "A versatile synthetic extracellular matrix mimic via thiol-norbornene photopolymerization," *Advanced Materials*, vol. 21, no. 48, pp. 5005–5010, 2009.

[44] H. Shih and C.-C. Lin, "Visible-light-mediated thiol-ene hydrogelation using eosin-y as the only photoinitiator," *Macromolecular rapid communications*, vol. 34, no. 3, pp. 269–273, 2013.

[45] S. K. Reddy, K. S. Anseth, and C. N. Bowman, "Modeling of network degradation in mixed step-chain growth polymerizations," *Polymer*, vol. 46, no. 12, pp. 4212 – 4222, 2005, in Honor of James E. Mark.

[46] C. N. Salinas and K. S. Anseth, "Mixed mode thiolacrylate photopolymerizations for the synthesis of pegpeptide hydrogels," *Macromolecules*, vol. 41, no. 16, pp. 6019–6026, 2008.

[47] P. J. Flory and J. Rehner Jr, "Statistical mechanics of cross-linked polymer networks swelling," *The Journal of Chemical Physics*, vol. 11, no. 11, pp. 521–526, 1943.

[48] J. Baier Leach, K. A. Bivens, C. W. Patrick Jr, and C. E. Schmidt, "Photocrosslinked hyaluronic acid hydrogels: natural, biodegradable tissue engineering scaffolds," *Biotechnology and bioengineering*, vol. 82, no. 5, pp. 578–589, 2003.

[49] T. Canal and N. A. Peppas, "Correlation between mesh size and equilibrium degree of swelling of polymeric networks," *Journal of Biomedical Materials Research*, vol. 23, no. 10, pp. 1183–1193, 1989.

[50] C. L. Bell and N. A. Peppas, "Water, solute and protein diffusion in physiologically responsive hydrogels of poly(methacrylic acid-g-ethylene glycol)," *Biomaterials*, vol. 17, no. 12, pp. 1203 – 1218, 1996.

[51] N. Peppas, P. Bures, W. Leobandung, and H. Ichikawa, "Hydrogels in pharmaceutical formulations," *European journal of pharmaceutics and biopharmaceutics*, vol. 50, no. 1, pp. 27–46, 2000.

[52] A. M. Atta and K.-F. Arndt, "Temperature and ph sensitive ionic hydrogels based on new crosslinkers," *Polymers for Advanced Technologies*, vol. 16, no. 6, pp. 442–450, 2005.

[53] S.-C. Chen, Y.-C. Wu, F.-L. Mi, Y.-H. Lin, L.-C. Yu, and H.-W. Sung, "A novel ph-sensitive hydrogel composed of carboxymethyl chitosan and alginate cross-linked by genipin for protein drug delivery," *Journal of Controlled Release*, vol. 96, no. 2, pp. 285 – 300, 2004.

[54] J. E. Elliott, M. Macdonald, J. Nie, and C. N. Bowman, "Structure and swelling of poly(acrylic acid) hydrogels: effect of ph, ionic strength, and dilution on the crosslinked polymer structure," *Polymer*, vol. 45, no. 5, pp. 1503 – 1510, 2004.

[55] S. J. Bryant, R. J. Bender, K. L. Durand, and K. S. Anseth, "Encapsulating chondrocytes in degrading peg hydrogels with high modulus: Engineering gel structural changes to facilitate cartilaginous tissue production," *Biotechnology and Bioengineering*, vol. 86, no. 7, pp. 747–755, 2004.

[56] S. R. Peyton, C. B. Raub, V. P. Keschrumrus, and A. J. Putnam, "The use of poly(ethylene glycol) hydrogels to investigate the impact of ecm chemistry and mechanics on smooth muscle cells," *Biomaterials*, vol. 27, no. 28, pp. 4881 – 4893, 2006.

[57] K. S. Anseth, C. N. Bowman, and L. Brannon-Peppas, "Mechanical properties of hydrogels and their experimental determination," *Biomaterials*, vol. 17, no. 17, pp. 1647 – 1657, 1996.

[58] C.-C. Lin and K. S. Anseth, *Biomaterials Science*. Elsevier Inc., Academic Press, 2013, ch. The biodegradation of biodegradable polymeric biomaterials, pp. 716–728.

[59] J. Zhu and R. E. Marchant, "Design properties of hydrogel tissue-engineering scaffolds," 2011.

[60] R. DeVolder and H.-J. Kong, "Hydrogels for in vivo-like three-dimensional cellular studies," *Wiley Interdisciplinary Reviews: Systems Biology and Medicine*, vol. 4, no. 4, pp. 351–365, 2012.

[61] A. E. Rydholm, C. N. Bowman, and K. S. Anseth, "Degradable thiol-acrylate photopolymers: polymerization and degradation behavior of an in situ forming biomaterial," *Biomaterials*, vol. 26, no. 22, pp. 4495 – 4506, 2005.

[62] B. D. Ulery, L. S. Nair, and C. T. Laurencin, "Biomedical applications of biodegradable polymers," *Journal of Polymer Science Part B: Polymer Physics*, vol. 49, no. 12, pp. 832–864, 2011.

[63] K. S. Anseth, A. T. Metters, S. J. Bryant, P. J. Martens, J. H. Elisseeff, and C. N. Bowman, "In situ forming degradable networks and their application in tissue engineering and drug delivery," *Journal of controlled release*, vol. 78, no. 1, pp. 199–209, 2002.

[64] J. M. Rhodes and M. Simons, "The extracellular matrix and blood vessel formation: not just a scaffold," *Journal of Cellular and Molecular Medicine*, vol. 11, no. 2, pp. 176–205, 2007.

[65] J. A. Burdick and K. S. Anseth, "Photoencapsulation of osteoblasts in injectable rgd-modified peg hydrogels for bone tissue engineering," *Biomaterials*, vol. 23, no. 22, pp. 4315 – 4323, 2002, injectable Polymeric Biomaterials.

[66] H. J. Lee, J.-S. Lee, T. Chansakul, C. Yu, J. H. Elisseeff, and S. M. Yu, "Collagen mimetic peptide-conjugated photopolymerizable peg hydrogel," *Biomaterials*, vol. 27, no. 30, pp. 5268 – 5276, 2006.

[67] C.-C. Lin and K. S. Anseth, "Glucagon-like peptide functionalized peg hydrogels promote survival and function of encapsulated pancreatic -cells," *Biomacromolecules*, vol. 10, no. 9, pp. 2460–2467, 2009, pMID: 19586041.

[68] K. T. Nguyen and J. L. West, "Photopolymerizable hydrogels for tissue engineering applications," *Biomaterials*, vol. 23, no. 22, pp. 4307–4314, 2002.

[69] J. P. Fisher, D. Dean, P. S. Engel, and A. G. Mikos, "Photoinitiated polymerization of biomaterials," *Annual review of materials research*, vol. 31, no. 1, pp. 171–181, 2001.

[70] S. J. Bryant and K. S. Anseth, *Scaffolding in tissue engineering*. CRC Press, 2005, ch. Photopolymerization of Hydrogel Scaffolds, pp. 71–90.

[71] B. D. Fairbanks, M. P. Schwartz, C. N. Bowman, and K. S. Anseth, "Photoinitiated polymerization of peg-diacrylate with lithium phenyl-2, 4, 6-trimethylbenzoylphosphinate: polymerization rate and cytocompatibility," *Biomaterials*, vol. 30, no. 35, pp. 6702–6707, 2009.

[72] A. A. Aimetti, A. J. Machen, and K. S. Anseth, "Poly(ethylene glycol) hydrogels formed by thiol-ene photopolymerization for enzyme-responsive protein delivery," *Biomaterials*, vol. 30, no. 30, pp. 6048 – 6054, 2009.

[73] U. P. Kappes, D. Luo, M. Potter, K. Schulmeister, and T. M. Rünger, "Short- and long-wave uv light induce similar mutations in human skin cells," *Journal of investigative dermatology*, vol. 126, no. 3, pp. 667–675, 2006.

[74] C. Kielbassa, L. Roza, and B. Epe, "Wavelength dependence of oxidative dna damage induced by uv and visible light." *Carcinogenesis*, vol. 18, no. 4, pp. 811–816, 1997.

[75] S. J. Bryant, C. R. Nuttelman, and K. S. Anseth, "Cytocompatibility of uv and visible light photoinitiating systems on cultured fibroblasts in vitro," *Journal of Biomaterials Science, Polymer Edition*, vol. 11, no. 5, pp. 439–457, 2000.

[76] T. Majima, W. Schnabel, and W. Weber, "Phenyl-2,4,6-trimethylbenzoylphosphinates as water-soluble photoinitiators," *Die Makromolekulare Chemie*, vol. 192, no. 10, pp. 2307–2315, 1991.

[77] C. S. Ki, H. Shih, and C.-C. Lin, "Facile preparation of photodegradable hydrogels by photopolymerization," *Polymer*, vol. 54, no. 8, pp. 2115 – 2122, 2013.

[78] S. Kzlel, V. H. Pérez-Luna, and F. Teymour, "Photopolymerization of poly(ethylene glycol) diacrylate on eosin-functionalized surfaces," *Langmuir*, vol. 20, no. 20, pp. 8652–8658, 2004, pMID: 15379488.

[79] C. Bahney, T. J. Lujan, C. Hsu, M. Bottlang, J. West, and B. Johnstone, "Visible light photoinitiation of mesenchymal stem cell-laden bioresponsive hydrogels," *European Cells and Materials*, vol. 22, pp. 43–55, 2011.

[80] M. P. Lutolf, G. P. Raeber, A. H. Zisch, N. Tirelli, and J. A. Hubbell, "Cell-responsive synthetic hydrogels," *Advanced Materials*, vol. 15, no. 11, pp. 888–892, 2003.

[81] A. T. Metters, C. N. Bowman, and K. S. Anseth, "A statistical kinetic model for the bulk degradation of pla-b-peg-b-pla hydrogel networks," *The Journal of Physical Chemistry B*, vol. 104, no. 30, pp. 7043–7049, 2000.

[82] E. Fournier, C. Passirani, C. Montero-Menei, and J. Benoit, "Biocompatibility of implantable synthetic polymeric drug carriers: focus on brain biocompatibility," *Biomaterials*, vol. 24, no. 19, pp. 3311 – 3331, 2003.

[83] A. T. Metters, K. S. Anseth, and C. N. Bowman, "A statistical kinetic model for the bulk degradation of pla-b-peg-b-pla hydrogel networks: Incorporating network non-idealities," *The Journal of Physical Chemistry B*, vol. 105, no. 34, pp. 8069–8076, 2001.

[84] M. V. Turturro and G. Papavasiliou, "Generation of mechanical and biofunctional gradients in peg diacrylate hydrogels by perfusion-based frontal photopolymerization," *Journal of Biomaterials Science, Polymer Edition*, vol. 23, no. 7, pp. 917–939, 2012.

[85] M. Lutolf, N. Tirelli, S. Cerritelli, L. Cavalli, and J. Hubbell, "Systematic modulation of michael-type reactivity of thiols through the use of charged amino acids," *Bioconjugate chemistry*, vol. 12, no. 6, pp. 1051–1056, 2001.

APPENDIX

APPENDIX: NMR SPECTRUM FOR SEVERAL PEG DERIVATIVES

A.1 PEG-tetra-acrylate

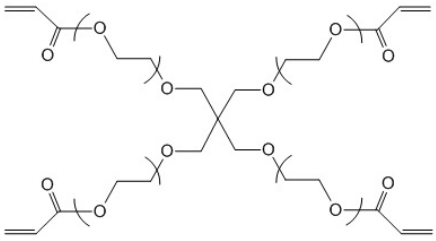

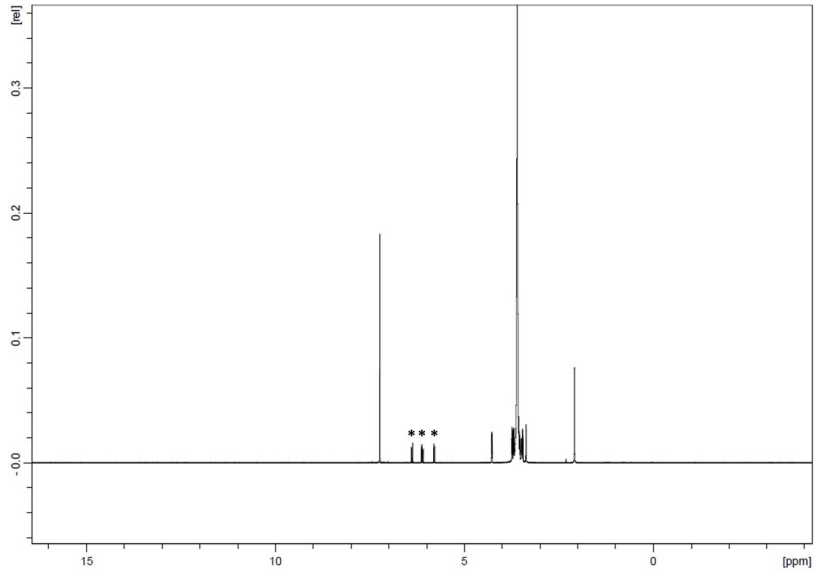

Chemical structure of PEG-tetra-acrylate and its H^1NMR spectrum.

Symbol $*$ represents hydrogen atoms in acrylate functional groups.

A.2 PEG-tetra-methacrylate

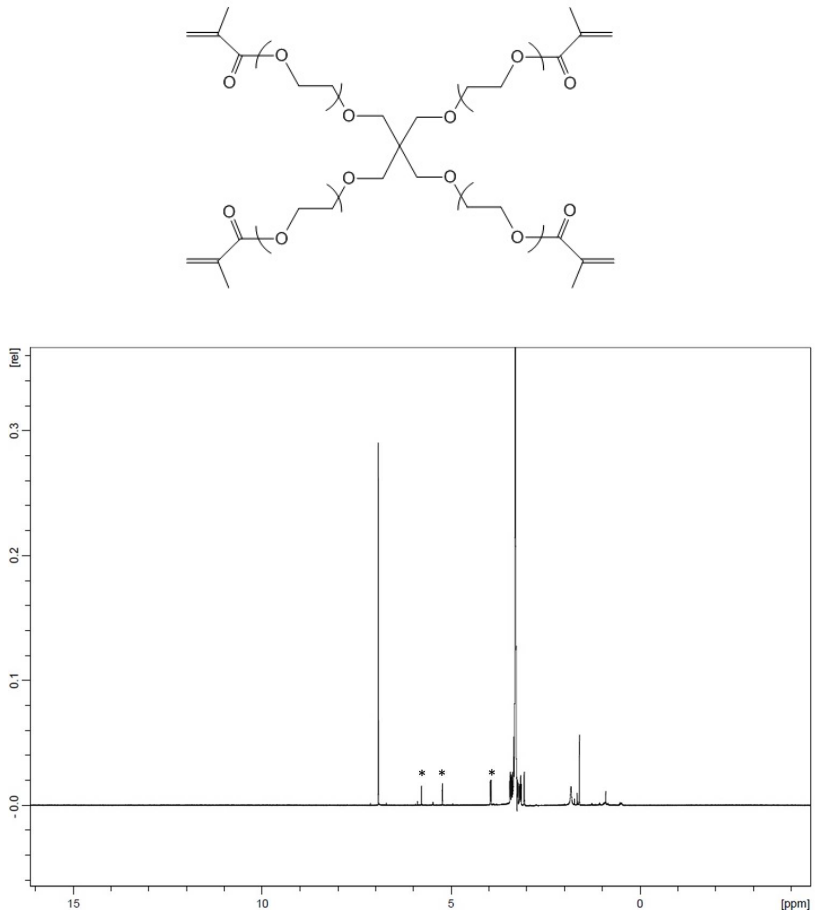

Chemical structure of PEG-tetra-methacrylate and its H^1NMR spectrum. Symbol $*$ represents hydrogen atoms in methacrylate functional groups.

A.3 PEG-tetra-acrylamide

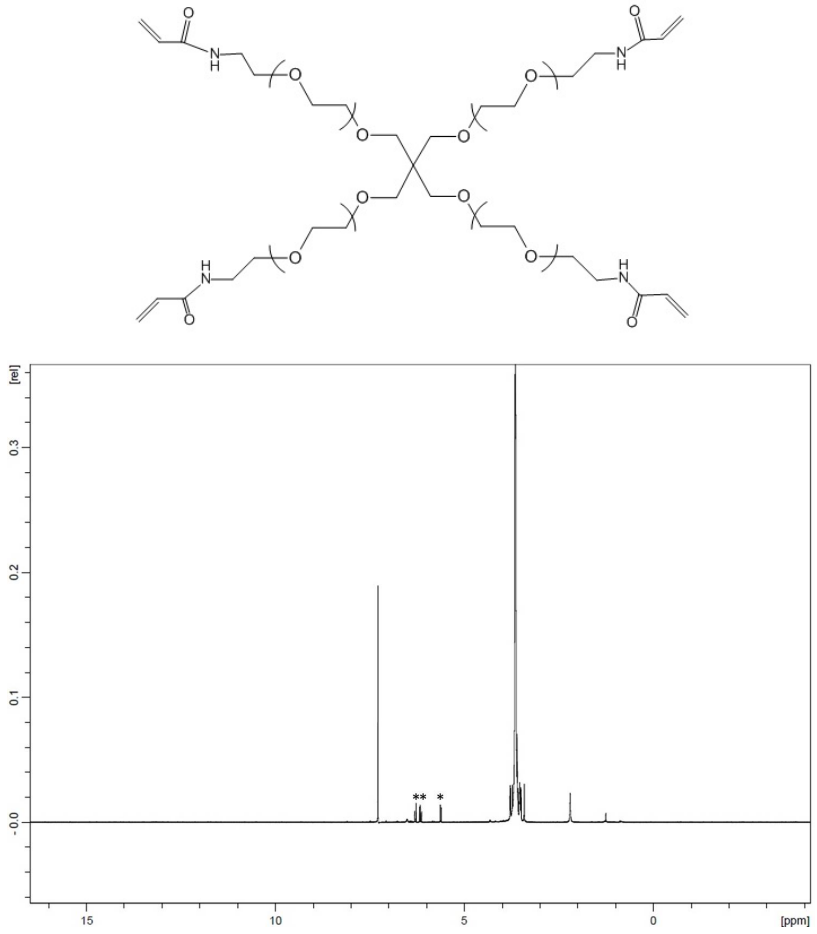

Chemical structure of PEG-tetra-acrylamide and its H^1NMR spectrum. Symbol $*$ represents hydrogen atoms in acrylamide functional groups.

A.4 PEG-tetra-allylther

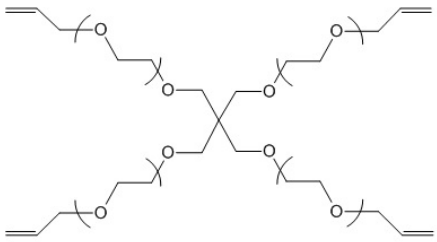

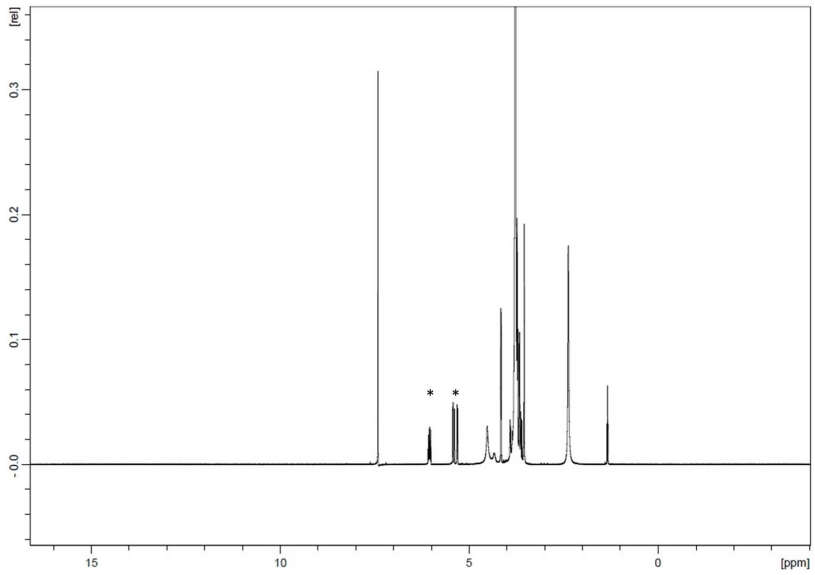

Chemical structure of PEG-tetra-allylther and its H^1NMR spectrum.
Symbol $*$ represents hydrogen atoms in allylther functional groups.